НАЦІОНАЛЬНА АКАДЕМІЯ НАУК УКРАЇНИ
ІНСТИТУТ ЗАГАЛЬНОЇ ТА НЕОРГАНІЧНОЇ ХІМІЇ імені В. І. ВЕРНАДСЬКОГО
КИЇВСЬКИЙ НАЦІОНАЛЬНИЙ УНІВЕРСИТЕТ імені ТАРАСА ШЕВЧЕНКА

УКРАЇНСЬКИЙ ХІМІЧНИЙ ЖУРНАЛ

№ 10
Том 87 / Vol. 87
2021
https://ucj.org.ua

UKRAINIAN CHEMISTRY JOURNAL

Зміст

ФІЗИЧНА ХІМІЯ

М. О. Марфунін, В. К. Клочков, П. М. Радіонов, М. О. Мчедлов-Петросян
ГІДРОЗОЛЬ ФУЛЕРЕНУ C_{70}: СИНТЕЗ ТА СТАБІЛЬНІСТЬ В ЕЛЕКТРОЛІТИЧНИХ РОЗЧИНАХ 63

Асєєва Д. А.
МЕТОДИ СИНТЕЗУ ТА ОСОБЛИВОСТІ ВИКОРИСТАННЯ СИСТЕМ НА ОСНОВІ МЕТАЛОКОМПЛЕКСІВ МОРІНУ У МЕТОДАХ ФЛУОРЕСЦЕНТНОГО АНАЛІЗУ 74

НЕОРГАНІЧНА ХІМІЯ

Трунова О. К., Артамонов М. С., Макотрик Т. О.
СПЕКТРОСКОПІЧНІ ДОСЛІДЖЕННЯ КОМПЛЕКСІВ Cu(II) ТА Co(II) З РУТИНОМ У РОЗЧИНІ 90

Смола С. С., Русакова Н. В., Алексеєва О. О., Басок С. С., Кіріченко Т. М., Коровін О. Ю., Малінка О. В., Семенішин М. М.
СТРУКТУРА ТА СПЕКТРАЛЬНО-ЛЮМІНЕСЦЕНТНІ ВЛАСТИВОСТІ ЛАНТАНІДВМІСНИХ КОМПЛЕКСІВ З АЗАКРАУН-КАЛІКСАРЕНАМИ 103

Contents

PHYSICAL CHEMISTRY

M. O. Marfunin, V. K. Klochkov, P. M Radionov, N. O. Mchedlov-Petrossyan
HYDROSOL OF C_{70} FULLERENE: SYNTHESIS AND STABILITY
IN ELECTROLYTIC SOLUTIONS 63

Asieieva D.A.
METHODS OF SYNTHESIS AND FEATURES OF USING SYSTEMS BASED ON
MORIN-METAL COMPLEXES IN FLUORESCENT ANALYSIS METHODS 74

INORGANIC CHEMISTRY

O.K. Trunova, M.S. Artamonov, T.O. Makotryk
SPECTROSCOPIC STUDIES OF Cu (II) AND Co (II) COMPLEXES WITH RUTIN
IN SOLUTIONS 90

Smola S.S., Rusakova N.V., Alekseeva O.A., Basok S.S., Kirichenko T.I., Korovin O.Yu., Malinka O.V., Semenyshyn N.N.
STRUCTURE AND SPECTRAL-LUMUINESCENT PROPERTIES OF LANTHANIDE-
CONTAINING COMPLEXES WITH AZACROWN CALIXARENES 103

УДК 544.77.05+546.26+544.353.3 doi: 10.33609/2708-129X.87.10.2021.63-73

HYDROSOL OF C_{70} FULLERENE: SYNTHESIS AND STABILITY IN ELECTROLYTIC SOLUTIONS

M. O. Marfunin,[a] V. K. Klochkov,[b] P. M. Radionov,[a] N. O. Mchedlov-Petrossyan[a]

[a] V. N. Karazin Kharkiv National University, 4 Svoboda sq., Kharkiv, 61022, Ukraine
[b] Institute for Scintillation Materials NAS of Ukraine, 61001 Kharkiv, Ukraine
e-mail: mchedlov@karazin.ua

This article is devoted to the synthesis and characterization of the C_{70} hydrosol of the son/nC_{70} type and to its coagulation by sodium chloride and cetyltrimethylammonium bromide (CTAB). At C_{70} concentration of 3.3×10^{-6} M, the electrokinetic potential is $\zeta = -40 \pm 4$ mV, the particle size expressed as Zeta-average is 97±3 nm; at higher C_{70} concentrations, 1.7×10^{-5} and 6.9×10^{-5} M, the size stays the same: 99 – 100 nm. The critical concentration of coagulation (CCC) values were determined using the diameter increasing rate (DIR) on NaCl concentration. The CCCs are concentration-dependent: 250, 145, and 130 mM at C_{70} concentrations 3.3×10^{-6}, 1.7×10^{-5}, and 6.9×10^{-5} M, respectively. The CCC for the CTAB surfactant is much lower, about 5×10^{-3} mM. At 0.02 mM CTAB, however, the overcharging up to $\zeta = +40$ mV and stabilization of the colloidal particles take place. Interpretation of the hydrosol coagulation by NaCl using the Derjaguin–Landau–Verwey–Overbeek theory makes it possible to determine the Hamaker constant of the C_{70}–C_{70} interaction in vacuum, if only electrostatic repulsion and molecular attraction are taking into account: $A_{FF} \approx 7\times10^{-20}$ J. On the other hand, if we use the value $A_{FF} = (16.0–16.6)\times10^{-20}$ J, obtained earlier in the study of organosols, then the data for hydrosols can be explained only by the introduction of an additional type of interactions. Following the terms of Churaev and Derjaguin, one should take into account the structural contribution to the interaction energy, which stabilizes the hydrosol.

Keywords: fullerene C_{70} hydrosol, electrokinetic potential, sodium chloride, cetyltrimethylammonium bromide, critical concentration of coagulation, Derjaguin – Landau – Verwey – Overbeek theory, Hamaker diagram, fullerene–fullerene Hamaker constant, structural contribution to the inter-particle interaction.

INTRODUCTION. The chemistry of fullerene solutions, including colloidal ones, is still one of the most interesting areas of nanoscience. Recent reviews give some idea of the current state of affairs in this area [1–3]. An important issue is the nature of aqueous suspensions and hydrosols of fullerenes [2]; the results of new detailed studies of these systems were published this year [4–6]. The last work [6] develops a previously published technique of preparation of the C_{60} hydrosol from the fullerene anion radical [7]. Another group of authors [8] published a molecular dynamics simulation study to understand the stabilization of fullerenes in water; the discussion was based on the idea of important role of the oxidized species $C_{60}O$, which was previously put forward by the Ausman's group [9].

During a study of C_{70} organosols in acetonitrile-based solvents and some other systems [10], as well as analogous dispersions of C_{60} [11, 12], we estimated the Hamaker constant, A_{FF}, of fullerene-fullerene interactions basing on the Derjaguin–Landau–Verwey–Overbeek (DLVO) theory. There are, however, two explanations of the data [10]. First one is based on averaging-out all the estimates obtained with different electrolytes. The average A_{FF} value is close to that estimated in aqueous systems [13–15], but the scatter is substantial. Alternatively, utilization of only several selected systems results in a substantially higher A_{FF} [10]. If the last value is accepted, the presence of a strong stabilizing factor in hydrosols should be presumed.

This paper is aimed to characterize the stability of the C_{70} hydrosol of the so-called son/nC_{70} type prepared by a somewhat modified procedure. Earlier Aich et al. [16, 17] studied in detail this hydrosol as well as those formed by C_{60}, C_{76}, and C_{84}. Values of the critical concentrations of coagulation of fullerene hydrosols and suspensions by electrolytes published in the literature were gathered in a review paper [2].

EXPERIMENT AND DISCUSSION OF THE RESULTS. Preparation of the C_{70} hydrosol. The first stage consisted in preparing a solution of fullerene in benzene. It is importantly to note that the water content in benzene should not exceed 0.01%. A weight amount of C_{70} (NeoTechProduct, >99%) was placed into benzene without intensive mixing; the final concentration was 5×10^{-4} M. The solution was stored for two weeks, stirring slowly every 3–5 days, and then filtered through a 0.22 μm membrane filter. The second stage was aimed to transfer the fullerene from benzene to water. In a 500 ml beaker, 400 ml of deionized water (conductivity $\leq$ 1.0 μS) was added and 30 ml of a C_{70} benzene solution (2.5×10^{-4} M) was added. The titanium tip of an ultrasonic disperser (22 kHz, 400–600 W) is immersed in the solution. Sonication was performed at reduced pressure of 100 mm. Hg. First, a white emulsion was formed. Then, the solution becomes transparent with brown tint. The solution thus obtained was centrifuged for 15–20 min at 7000–8000 rpm in order to remove the titanium particles and the coarse fraction of C_{70} particles. The supernatant part of the solution is placed in a round-bottomed flask of a rotary evaporator and evaporated at a bath temperature of 65 °C to 12 – 15 ml. Then the solution is filtered through membrane filters with pore diameters of 0.45 and 0.22μm. The result is a clear dark brown solution containing $(6–8)\times10^{-4}$ M C_{70}.

Determination of the fullerene concentration and molar absorptivity in water. 2 ml of C_{70} aqueous solution are placed in a 10 ml eva-

porating flask and evaporated to dryness on a rotary evaporator. Then, 2 ml of a mixture of water/acetone in a ratio of 1: 1 are poured into the flask and evaporated to dryness. Then 2 ml of acetone is poured into the flask twice and each time is evaporated to dryness. After drying and removing traces of acetone, 2 ml of benzene are placed in the flask and left to dissolve completely. The concentration of the fullerene in the hydrosol, 4.30×10^{-4} M, was estimated using the molar absorptivity of C_{70} in benzene, 44.7×10^{3} $M^{-1}cm^{-1}$, at 382.1 nm. {The molar absorptivity in benzene was estimated by 100-fold dilution by highly purified toluene and using the molar absorptivity of C_{70} in toluene used previously [10]}. Then, the molar absorptivity of C_{70} in the hydrosol at 385.7 nm was estimated as 48.0×10^{3} $M^{-1}cm^{-1}$. The absorption spectra are presented in Figure 1.

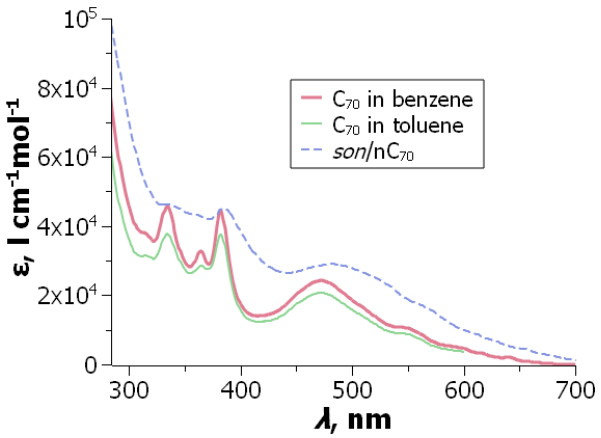

Figure 1 – UV/visible absorption spectra of C_{70} in different media.

This spectrum of the hydrosol is very similar to those reported by Aich et al. [16, 17] and Mikheev et al. [18].

Other chemicals. To determine the hydrosols CCC, the solutions of NaCl (analytical grade) and cetriltrimethylammonium bromide (CTAB, 99 %, Sigma-Aldrich) were used. These solutions were prepared by dissolving of required salt amount in distillate water.

Preparation of the working solutions. The required amount of electrolyte solution was added to the flask, then distillate water. After mixing, an aliquot of the C_{70} stock solution was added to the flask and the solution was stirred again.

Apparatus. UV/visible spectra were run with a Hitachi U-2000 spectrophotometer against solvent blanks. Particle size distribution was obtained using dynamic light scattering via Zetasizer Nano ZS Malvern Instruments, scattering angle 173°; each measurement was made by 12 runs and reproduced at least three times. The values of the ζ-potentials were determined using the Zetasizer Nano ZS Malvern Instruments, scattering angle 12.8°; each measurement was performed by 3–5 runs. The spectral and DLS measurements were made at 25.0±0.5 °C.

Characterization of the hydrosols. Particle size distribution at different fullerene concentrations is presented in Figure 2.

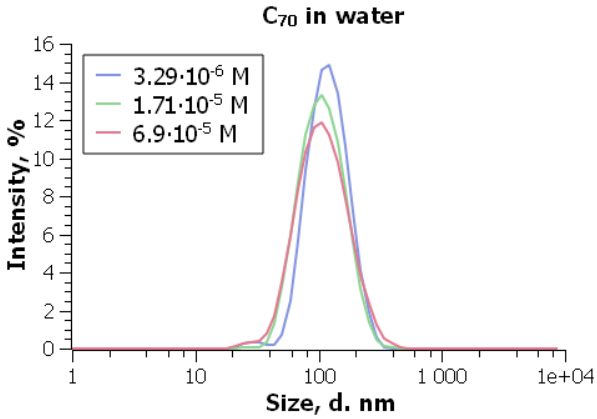

Figure 2 – Particle size distribution of the son/nC_{70} hydrosol at various dilutions of the initial sol.

Main experiments were processed with the concentration of 3.29×10^{-6} M C_{70}. The particles are negatively charged, ς = –40 ± 4 mV. The Z-average value is d = 97 ± 3 nm (by number 51 nm; by volume 60; by intensity 110; PDI = 0.18). For C_{70} concentration of 1.71×10^{-5} M, Z-average is 99 nm; the size by number, volume, and intensity is 51; 63; and 114 nm, and PDI = 0.18. For 6.91×10^{-5} M C_{70}, the corresponding values are 100 nm; 51; 59; and 120 nm, PDI = 0.22. All the values of the zeta-potential presented here are calculated using the Ohshima equation [19, 20]; in salt-free water, this corresponds to the Onsager–Hückel equation. Note, that other authors [15, 16, 18, 21] use the Smoluchowsky equation.

Aich et al. report the hydrodynamic diameter of 92 ± 14 nm and ς= –39 ± 4 mV [15], Mikheev et al. [18] report d = 175±5 nm (PDI = 0.11±0.02), ς= –34.4 ± 0.7 mV (measurements at 6.2×10^{-5} M C_{70}).

Coagulation by sodium chloride. The critical coagulation concentration was determined using the dependence of the diameter increasing rate (DIR) on NaCl concentration (Figure 3), which is in fact a sort of the Fuchs approach [10–15, 17].

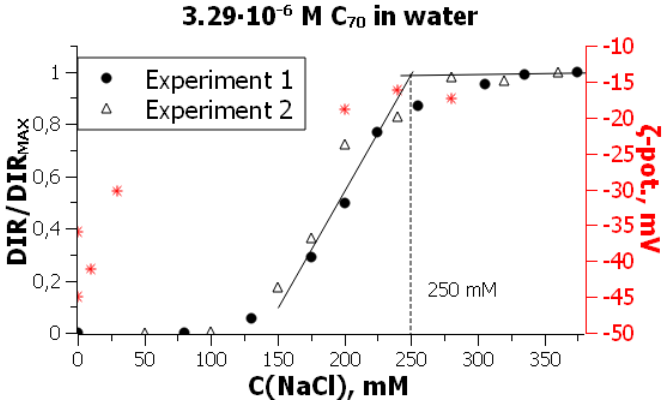

Figure 3 – Determination of the critical coagulation concentration of the C_{70} hydrosol by NaCl: the results of two independent experiments; asterisks indicate the ς values.

The CCC value at 3.3×10^{-6} M C_{70} is 250 mM NaCl. Increasing in the fullerene concentration up to 1.71×10^{-5} M decreases the CCC value down to 145 mM. This is in line with the results obtained with C_{60} hydrosols [2]. Further rise of C_{70} concentration to 6.91×10^{-5} M also decreases the CCC to 130 mM. However, the system is unstable under such conditions, and the coagulation occurs in spurts. Note, that at 1×10^{-4} M of C_{60} hydrosol CCC = 85 mM NaCl (determined by visual titration) [22]. Aich et al. [17] reported a CCC value of 150 mM at 7.9×10^{-7} M C_{70} (the fullerene concentration was calculated using the information on the experimental details kindly sent to us by Dr. Aich).

Interaction of the C_{70} hydrosol particles with CTAB. Small concentrations of CTAB cause charge neutralization of the particles and coagulation of the hydrosol; the size jump approximately corresponds to the isoionic state (Figure 4). The CCC value is about 0.005 mM CTAB. In contrast, further increase in CTAB concentration results in overcharging and

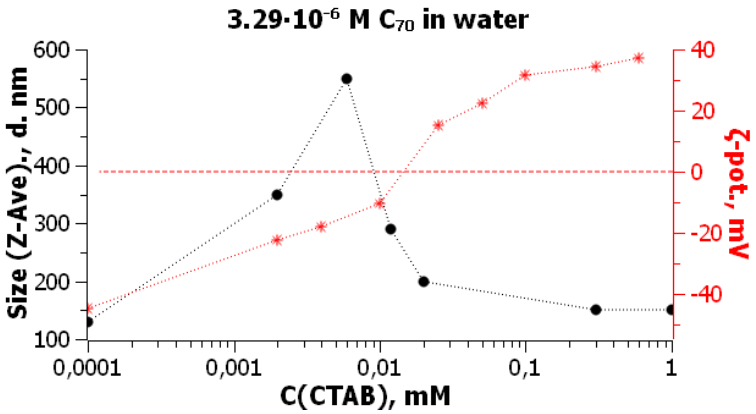

Figure 4 – Size and zeta-potential dependence of the C_{70} colloid in CTAB solutions; asterisks indicate the ς values.

thus stabilization of the sol. This phenomenon is typical for colloidal systems, e.g., for the SiO_2/CTAB [23]. Whereas the coagulation within the range of micromolar CTAB concentrations is obviously caused by adsorption and hence charges neutralization of colloidal particles, the stabilization via particles overcharging is probably a result of surfactant bilayer formation [22, 24].

Interpretation of the CCC(NaCl) value. Despite some differences of the CCCs determined at various C_{70} concentrations and by different authors, these values as well as those for C_{60} hydrosol [2, 13-15, 17, 18, 21, 22], are two-three orders of magnitude higher as compared with the values in organic solvents [10–12]. In both cases, attempts were made to estimate the fullerene–fullerene Hamaker constant, A_{FF}, which characterizes the C_{70}–C_{70} interaction in vacuum, selecting in one way or another a value consistent with a given coagulation threshold. For example, an equation derived by Dukhin et al. [25] can be used, Eq. 1.

$$U = U_{el} + U_{attr} = 64\pi\varepsilon_r\varepsilon_0\left(\frac{RT}{F}\right)^2 \mathrm{tgh}^2\left(\frac{\Psi_d F}{4RT}\right)\frac{r\exp(-\kappa h)}{s} - \frac{A^*_{FSF}}{6}\left[\frac{2}{s^2-4}+\frac{2}{s^2}+\ln\frac{s^2-4}{s^2}\right] \quad (1)$$

Here, h is the distance between the centers of the particles, $s = 2 + h/r$, Ψ_d is the electrical surface potential of the colloidal particles, $\varepsilon_0 = 8.854\times10^{-12}$ F m^{-1}, κ is the reciprocal Debye length, R, T, F have their usual meanings. The measured values of ς can be used for low and medium charged interfaces instead of Ψ_d, in accord to the accepted viewpoint. The A^*_{FSF} value characterizes the fullerene – solvent – fullerene interaction in solution and is connected with the A_{FF} and A_{SS} values, which characterize the fullerene–fullerene and solvent–solvent interactions in vacuum, respectively, through Eq. 2.

$$A^*_{FSF} = (A_{FF}^{1/2} - A_{SS}^{1/2})^2. \quad (2)$$

Different dependences of U on h can be constructed using various A^*_{FSF} values, and those which meet the coagulation conditions should be selected. Accordingly, the A_{FF} can

be estimated using Eq. 2. In our recent work, in this way we estimated the A^*_{FSF} and A_{FF} values for C_{70} in acetonitrile and methanol (with 10 vol. % toluene) [10]. Using the data for a set of electrolytes, we obtained the A_{FF} values within a wide range of (5.8 – 16.6)×10^{-20} J [10]; similar A_{FF} were estimated for C_{60} in acetoni-trile and methanol [11, 12].

At the same time, Elimelech and his co-workers obtained the value A_{FF} = 7.5×10^{-20} J for C_{60} hydrosols prepared by different procedures [13, 15]. Aich et al. [17] used this value for successful explanation of the coagulation of aqueous suspensions of C_{60}, C_{70}, C_{76}, and C_{84}. Therefore, the data obtained with organosols can be considered as an approximate estimate, with the value 7.5 × 10^{-20} J falling within this range.

However, an alternative explanation can be proposed. A careful consideration of the data for organosols demonstrates an expressed tendency to overcharging of the negatively charged colloidal particles of the fullerenes by the metal cations. This most likely leads to hetero- and mutual coagulation, and the simple interpretation of the CCCs using Eq. 1 becomes impossible. Therefore, we selected the data for two electrolytes as coagulators in organic solvents. They are as follows: tetra-*n*-butylammonim perchlorate, chosen because of no signs of overcharging, and calcium perchlorate, which exhibits a second CCC value for completely overcharged C_{70} aggregates [10]. This allows estimating the A_{FF} value (16.0 – 16.6) ×10^{-20} J [10], which is substantially higher as compared with the "aqueous" value, A_{FF} = 7.5×10^{-20} J. This, in turn, allows suspecting the presence of an additional stabilizing factor in the case of the hydrosols [10].

In Figure 5, series of Hamaker diagrams are presented for ionic strength of 250 mM and ς = –17 mV, i.e., under conditions of rapid coagulation by NaCl (see above), and different A^*_{FSF} values; A_{SS} for water is 3.86×10^{-20} J.

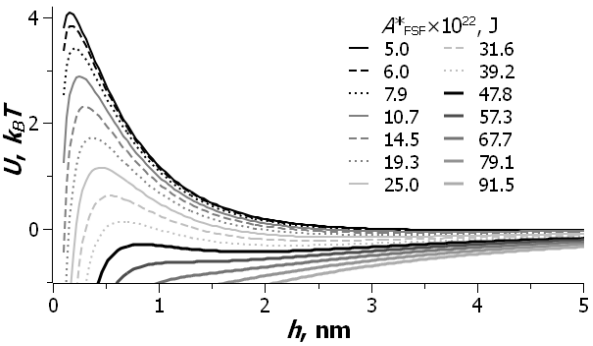

Figure 5 – Hamaker diagrams for the C_{70} hydrosol for 250 mM NaCl.

In Figure 6, the U_{max} values in k_BT units are plotted against the A^*_{FSF} values.

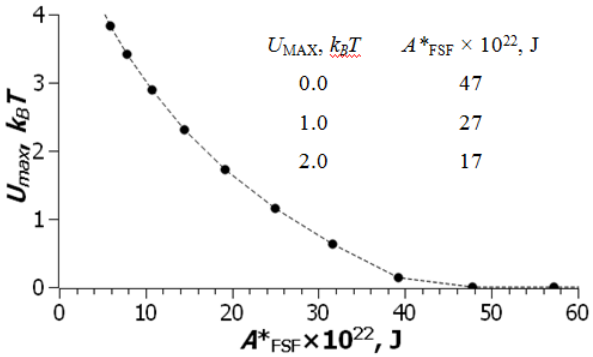

Figure 6 – Potential barrier height as a function of the Hamaker constant.

If the values of the potential barrier U_{max} = (0 – 1) k_BT are accepted as the margin of the stability, then A_{FF} = (7.0 to 6.2)×10^{-20} J (Table 1). Average value is 6.6×10^{-20} J; for U_{max} = 0, A_{FF} = 7.0×10^{-20} J.

Table 1

Calculated values of the Hamaker constant.

U_{max}, k_BT	A^*_{FSF}, 10^{-20} J	A_{FF}, 10^{-20} J
0.00	0.47	7.02
1.00	0.27	6.17
2.00	0.17	5.65
Mean	0.30	6.3

These estimates are in line with the above mentioned publications [13, 15]. On the other hand, if we use the "refined" data obtained from the examination of organosols, A_{FF} = (16.0 to 16.6)×10^{-20} J, then the picture changes radically. In Figure 7, the Hamaker diagrams are constructed with these values. For ionic strength of 100 mM, ζ = –22 mV and the DIR value is low but not zero (heavy curve). Here, as well as for higher NaCl concentrations, the system would have to be completely unstable, while experimentally the slow coagulation is observed (Figure 3). At 30 mM NaCl, where the system is quite stable (ζ = –30 mV, DIR approaches zero), the barrier height is about 0.5 k_BT (light curves, built for several A_{FF} values from 16.0×10^{-20} J to 16.6×10^{-20} J). Thus, here the rapid coagulation can be expected, which is, however, not the case (Figure 3).

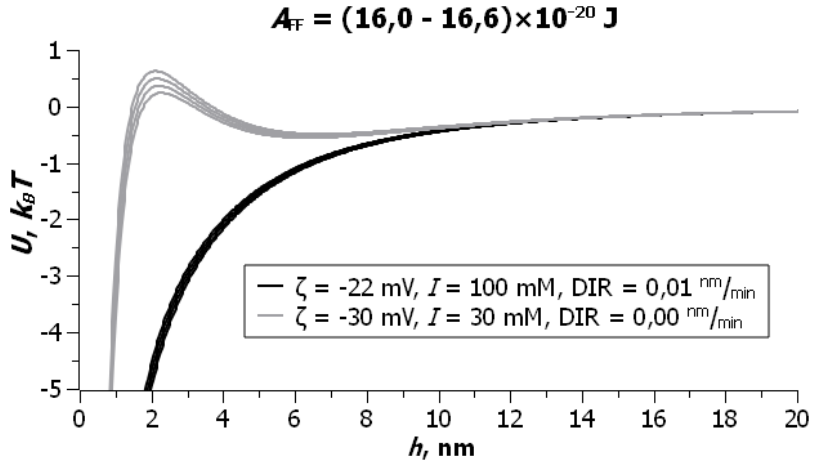

Figure 7 – Hypothetical Hamaker diagrams based on molecular attraction, A_{FF} = (16.0 to 16.6)×10^{-20} J, and electrostatic repulsion.

Therefore, the experimental CCC is ca. one order of magnitude higher than the predicted threshold calculated with the A_{FF} values estimated in organic solvents. As it was mentioned above, an interaction that stabilizes the hydrosol should be expected. According to Derjaguin and Churaev, a structural (hydration) contribution to the disjoining pressure must be taken into account [26]. In other words, the U value in Eq. 1 may contain an additional quantity, U_s , Eq. (3).

$$U_s = Kl\exp(-h/l)\,. \qquad (3)$$

Here K and l are constants; for hydrophilic and hydrophobic surfaces, $K > 0$ (structural repulsion) and $K < 0$ (structural attraction), respectively. Without knowing the two constants, K and l, it is difficult to draw precise

quantitative conclusions. In fact, the additional contribution, U_s , is opposed to the second item of the rhs of Eq. 1, but the type of the function is exponential. Approximate estimation for $A_{FF} = 7.0\times10^{-20}$ J is as follows: at 30 mM NaCl and $\varsigma = -30$ mV, the U_{max} value is 26 k_BT. This value is much higher than that given in Figure 7. If the U value is compared at the distance, which corresponds to the barrier maximum in Figure 7, the difference is around 13 k_BT. In any case, the model proposed in the present paper looks out as self-consisted. This also is in line with numerous reports devoted to specific fullerene–water interactions [2, 10, 27–31].

CONCLUSIONS. The C_{70} hydrosol prepared by solvent-exchange method (a system of the son/nC_{70} type) is characterized by a electrokinetic potential of –40 ± 4 mV and particle size 97±3 nm at fullerene concentration of 3.3×10^{-6} M. The critical concentrations of coagulation (CCC) values are decreasing from 250 to 130 mM NaCl along with the rise of the hydrosol concentration from 3.3×10^{-6} to 6.9×10^{-5} M. The CCC for the CTAB surfactant is about 5×10^{-3} mM, i.e., fifty thousand times lower. Higher CTAB concentrations lead to overcharging of the colloidal particles up to $\zeta = +40$ mV and stabilization of the hydrosol.

Using the DLVO theory to explain the coagulation of the hydrosol by NaCl allows determining the Hamaker constant of the C_{70}–C_{70} interaction in vacuum, if only electrostatic repulsion and molecular attraction are taking into account: $A_{FF} \approx 7\times10^{-20}$ J. On the other hand, if the value $A_{FF} = (16.0–16.6)\times10^{-20}$ J, obtained earlier during the study of organosols, is used, then the data for hydrosols can be explained only by taking into account an additional type of interactions. Following the terms of Churaev and Derjaguin, one should take into account the structural contribution to the interaction energy, U_s , which stabilizes the hydrosol.

ACKNOWLEDGMENTS

This study was partly supported by the Ministry of Education and Science of Ukraine, grant 0119U002532. The authors express their gratitude to Dr. Nirupam Aich, University at Buffalo, USA, for informing about some details of his experiments reported in ref. [16, 17].

ГІДРОЗОЛЬ ФУЛЕРЕНУ C_{70}: СИНТЕЗ ТА СТАБІЛЬНІСТЬ В ЕЛЕКТРОЛІТИЧНИХ РОЗЧИНАХ

М. О. Марфунін,[1] В. К. Клочков,[2] П. М. Радіонов,[1] М. О. Мчедлов-Петросян[1]

[1]Харківський національний університет імені В. Н. Каразіна, пл. Свободи, 4, Харків 61022, Україна

[2]Інститут сцинтиляційних матеріалів НАН України, Харків 61001, Україна

e-mail: mchedlov@karazin.ua

Статтю присвячено синтезу та характеризації гідрозолю C_{70} і його коагуляції хлоридом натрію та бромідом цетилтриметиламонію (CTAB). При концентрації C_{70} 3.3×10^{-6} М електрокінетичний потенціал дорівнює $\zeta = -40 \pm 4$ мВ, а розмір колоїдних частинок, виражений як Zeta-average,

дорівнює 97±3 нм; при концентраціях C_{70} 1.7×10^{-5} і 6.9×10^{-5} М розмір частинок залишається таким же: 99–100 нм. Значення критичної концентрації коагуляції (ССС) було визначено, використовуючи залежність швидкості зростання діаметру від концентрації NaCl. Значення ССС залежать від концентрації гідрозолю: вони дорівнюють 250, 145 і 130 мМ при концентраціях C_{70} 3.3×10^{-6}, 1.7×10^{-5} і 6.9×10^{-5} М, відповідно. Значення ССС при коагуляції за допомогою CTAB є набагато нижчим: $\approx 5\times10^{-3}$ мМ. Але при концентрації CTAB 0.02 мМ спостерігаємо перезарядження до ζ = + 40 мВ і стабілізацію колоїдних частинок. Інтерпретація коагуляції гідрозолю хлоридом натрію за допомогою теорії ДЛФО робить можливим оцінку константи Гамакера для взаємодії C_{70}–C_{70} у вакуумі, $A_{FF} \approx 7\times10^{-20}$ Дж, якщо враховувати тільки електростатичне відштовхування та молекулярне притягання. З іншого боку, якщо використовувати значення A_{FF} = (16.0–16.6)$\times10^{-20}$ J, знайдене раніше при вивченні органозолів, тоді результат для гідрозолю стає можливим тільки при введенні до розгляду додаткового типу взаємодій. Згідно з Чураєвим і Дерягіним, треба враховувати внесок структурної складової до загальної енергії взаємодії, який стабілізує гідрозоль.

Keywords: гідрозоль фулерену C_{70}, електрокінетичний потенціал, хлорид натрію, бромід цетилтриметиламонію, критична концентрація коагуляції, теорія Дерягіна – Ландау – Вервея – Овербека, діаграма Гамакера, константа Гамакера фулерен – фулерен, структурний внесок у взаємодію між частинками.

REFERENCES

1. Kyzyma O. A. Liquid systems with fullerenes in organic solvents and aqueous media. *Ukrainian J. Phys.* 2020. **65** (9): 761–767. https://doi.org/10.15407/ujpe65.9.761
2. Mchedlov-Petrossyan N.O. Fullerenes in aqueous media: A review. *Theoretical and Experimental Chemistry*. 2020. **55** (6): 361–391. https://doi.org/10.1007/s11237-020-09630-w
3. Kharissova O. V., Oliva González C. M., Kharisov B.L. Solubilization and Dispersion of Carbon Allotropes in Water and Non-Aqueous Solvents. *Industrial & Engineering Chemistry Research.* 2018. **57** (38): 12624–12645. https://doi.org/10.1021/acs.iecr.8b02593
4. Mikheev I. V., Sozarukova M. M., Izmailov D. Yu., Kareev I. E., Proskurnina E. V., Proskurnin M. A. Antioxidant Potential of Aqueous Dispersions of Fullerenes C_{60}, C_{70}, and Gd@C_{82}. *International Journal of Molecular Sciences* 2021. **22** (5838): 1–13. https://doi.org/10.3390/ijms22115838
5. Mikheev I. V., Pirogova M. O., Usoltseva L. O., Uzhel A. S., Bolotnik T. A., Kareev I. E., Bubnov V. P., Lukonina N. S., Volkov D. S., Goryunkov A. A., Korobov M. V., Proskurnin M. A. Green and rapid preparation of long-term stable aqueous dispersions of fullerenes and endohedral fullerenes: The pros and cons of an ultrasonic probe. *Ultrasonics Sonochemistry.* 2021. **73**: 105533. https://doi.org/10.1016/j.ultsonch.2021.105533
6. Damasceno J. P. V., Hof F., Chauvet O., Zarbin A. J. G., Pénicaud A. The role of functionalization on the colloidal stability of aqueous fullerene C_{60} dispersions prepared with fullerides. *Carbon*. 2021. **173**: 1041–1047. https://doi.org/10.1016/j.carbon.2020.11.082
7. Wei X., Wu M., Qi L., Xu Z., Selective solution-phase generation and oxidation reaction of C_{60}^{n-} (n = 1,2) and formation of an aqueous colloidal solution of C_{60}. *J. Journal of the Chemical Society, Perkin Transactions 2*. 1997. 1389–1394. https://doi.org/10.1039/a607336k

8. Noneman K., Muhich C., Ausman K., Henry M., Jankowski E. Molecular simulations for understanding the stabilization of fullerenes in water. *Journal of Computational Science Education*. 2021. **12** (1): 39–48 https://doi.org/10.22369/issn.2153-4136/12/1/6
9. Murdianti B. S., Damron J. T., Hilburn M. E., Maples R. D., HikkaduwaKoralege R. S., Kuriyavar S. I., Ausman K. D. C_{60} Oxide as a Key Component of Aqueous C_{60} Colloidal Suspensions. *Environmental Science & Technology*. 2012. **46:** 7446–7453. https://dx.doi.org/10.1021/es2036652
10. Mchedlov-Petrossyan N. O., Marfunin M. O. Formation, Stability, and Coagulation of Fullerene Organosols: C_{70} in Acetonitrile–Toluene Solutions and Related Systems. *Langmuir*. 2021. **37** (23): 7156–7166. https://doi.org/10.1021/acs.langmuir.1c00722.
11. Mchedlov-Petrossyan N. O., Al-Shuuchi Y. T. M., Kamneva N. N., Marynin A. I. , Klochkov V. K. The Interactions of the Nanosized Aggregates of Fullerene C_{60} with Electrolytes in Methanol: Coagulation and Overcharging of Particles. *Langmuir*. 2016. **32** (39): 10065–10072. http://dx.doi.org/10.1021/acs.langmuir.6b02533
12. Mchedlov-Petrossyan N. O., Kamneva N. N., Al-Shuuchi Y. T .M., Marynin A. I. Interaction of C_{60} aggregates with electrolytes in acetonitrile. *Colloids and Surfaces A: Physicochemical and Engineering Aspects.* 2017. **516**: 345–353. http://dx.doi.org/10.1016/j.colsurfa.2016.12.035
13. Chen K. L., Elimelech M. Aggregation and deposition kinetics of fullerene (C_{60}) nanoparticles. *Langmuir.* 2006. **22** (26): 10994–11001. https://doi.org/10.1021/la062072v
14. Chen K. L., Elimelech M. Relating colloidal stability of fullerene (C_{60}) nanoparticles to nanoparticle charge and electrokinetic properties. *Environmental Science & Technology*. 2009. **43** (19): 7270–7276. https://doi.org/10.1021/es900185p
15. Meng Z., Hashmi S. M., Elimelech M. Aggregation rate and fractal dimension of fullerene nanoparticles via simultaneous multiangle static and dynamic light scattering measurement. *Journal of Colloid and Interface Science.* 2013. **392**: 27–33. https://doi.org/10.1016/j.jcis.2012.09.088
16. Aich N., Flora J. R. V., Saleh N. B. Preparation and characterization of stable aqueous higher-order fullerenes. *Nanotechnol.* 2012. **23** (055705): 1–9. http://doi.org/10.1088/0957-4484/23/5/055705
17. Aich N., Boateng L. K., Sabaraya I. V. Das D., Flora J. R. V., Saleh N. B. Aggregation Kinetics of Higher-Order Fullerene Clusters in Aquatic Systems. *Environmental Science & Technology.* 2016. **50** (7): 3562–3571. https://doi.org/10.1021/acs.est.5b05447
18. Mikheev I. V., Bolotnik T. A., Volkov D. S., Korobov M.V., Proskurnin M. A. Approaches to the determination of C_{60} and C_{70} fullerene and their mixtures in aqueous and organic solutions. *Nanosystems: Physics, Chemistry, Mathematics.* 2016. **7** (1): 104–110. https://doi.org/10.17586/2220-8054-2016-7-1-104-110
19. Delgado A. V., González-Caballero F., Hunter R. J., Koopal L. K., Lyklema J. Measurement and interpretation of electrokinetic phenomena. *Journal of Colloid and Interface Science* 2007. **309**: 194–224 https:/doi.org/10.1016/j.jcis.2006.12.075
20. Ohshima H. A simple expression for Henry's function for the retardation effect in electrophoresis of spherical colloidal particles. *Journal of Colloid and Interface Science* 1994. **168**: 269–271. https://doi.org/10.1006/jcis.1994.1419
21. Михеев И. В. Дисс. … канд. хим. наук. Москва: МГУ, 2018.
22. Mchedlov-Petrossyan N. O., Klochkov V. K., Andrievsky G. V. Colloidal dispersions of fullerene C_{60} in water: some properties and regularities of coagulation by electrolytes. *Journal of the Chemical Society, Faraday Transactions*. 1997. **93** (24): 4343–4346. https://doi.org/10.1039/A705494G
23. Wang W., Gu B., Liang L., Hamilton W.B.

Adsorption and Structural Arrangement of Cetyltrimethylammonium Cations at the Silica Nanoparticle–Water Interface. *Journal of Physical Chemistry B*. 2004. **108** (45): 17477–17483. https://doi/10.1021/jp048325f

24. Gigault, J., Budzinski, H. Selection of An Appropriate Aqueous Nano-Fullerene (nC_{60}) Preparation Protocol for Studying its Environmental Fate and Behavior, *Trends In Analytical Chemistry*. 2016. **80**: 1–11. https://doi.org/10.1016/j.trac.2016.02.019
25. Dukhin S. S.; Derjaguin B. V.; Semenikhin N. M. The interaction of two identical spherical colloidal particles in large distances (in Russian). *Doklady AN USSR*. 1970. **192**: 357–360.
26. Churaev N. V., Derjaguin B.V., Inclusion of structural forces in the theory of stability of colloids and films. *Journal of Colloid and Interface Science*. 1985. **103**: 542–553. https://doi.org/10.1016/0021-9797(85)90129-8
27. Brant J. A., Labille J., Bottero J.-Y., Wiesner M. R. Characterizing the impact of preparation method on fullerene cluster structure and chemistry. *Langmuir*. 2006. **22**: 3878–3885. https://doi.org/10.1021/la053293o
28. Ma X., Wiginton B., Bouchard D. Fullerene C_{60}: Surface energy and interfacial interactions in aqueous systems. *Langmuir*. 2010. **26**: 11886–11893. https://doi.org/10.1021/la101109h
29. Choi J. I., Snow S. D., Kim J.-H., Jang S. S., Interaction of C_{60} with water: first-principles modeling and environmental implications. *Environ. Sci. Technol*. 2015. **49**: 1529–1536. https://doi.org/10.1021/es504614u
30. Li L., Bedrov D., Smith G. D., A molecular-dynamics simulation study of solvent-induced repulsion between C_{60} fullerenes in water. *J. Chem. Phys*. 2005. **123**: No. 204504. https://doi.org/10.1063/1.2121647
31. Bedrov D., Smith G. D., Davande H., Li L. Passive transport of C_{60} fullerenes throuhj a lipid membrane: A molecula dynamics simulation study. *J. Phys. Chem. B* 2008. **112:** 2078–2084. https://doi.org/10.1021/jp075149c

Стаття надійшла 25.11.2021.

UDC 546.05+546.06 doi: 10.33609/2708-129X.87.10.2021.74-89

METHODS OF SYNTHESIS AND FEATURES OF USING SYSTEMS BASED ON MORIN-METAL COMPLEXES IN FLUORESCENT ANALYSIS METHODS

***Asieieva D.A.*[1,2]**

[1]*Université Toulouse III - Paul Sabatier, 118 route de Narbonne, Toulouse Cedex, 9, 31062, France*
[2]*Taras Shevchenko National University of Kyiv, Volodymyrska St, 60, Kyiv 01033, Ukraine*
email: dasha.aseeva@gmail.com

The review describes modern physicochemical systems based on complex compounds with organic ligands, which may have fluorescent properties when interacting with metal ions or proteins. Modern methods of synthesis of these compounds and their use in physical-chemical methods of analysis are given. Approaches to detecting the content of metals and proteins using the fluorescent properties of morin complex compounds are considered. Areas of use of the effects of amplification and quenching of fluorescence for the determination of organic compounds and metal ions, especially in the presence of DNA and RNA of different biological origin are described. The influence of surfactants on the fluorescence intensity of complexes with morin was analyzed separately.

Key words: morin, complex compounds, fluorescence, analysis, metal ions, protein.

INTRODUCTION. Physical-chemical methods using fluorescent materials make it possible to solve various scientific and applied problems in the field of chemistry, physics, biology, environmental monitoring and medical diagnostics due to high sensitivity, selectivity and expressiveness [1]. It is noteworthy that in many cases the use of micellar systems leads to an increase in the intensity of fluorescence and quantum yields by more than two orders of magnitude, and, accordingly, to a decrease in the detection limits of analytes. Surfactants have specific and sometimes unique properties. They are not only analytical reagents, but also able to effectively affect the physicochemical properties of other substances in solutions, such as proteins [2, 3], which are involved in building muscle tissue, as well as parts of the hair, nails and internal bodies. Therefore, qualitative and quantitative analysis of proteins is important in clinical trials and applications [4–6]. Therefore, the development of new physical-chemical methods and selection of conditions for the rapid determination of microquantities of protein is very relevant today. In addition, fluorescent properties can be

used in the development of labeling reagents for the further development of such methods as: high performance liquid chromatography, spectrophotometry and selective sensors [7–9]. For the development of these methods, the conditions for the synthesis of reagents and their organic component are of great importance, which in many cases is the key to the substance's acquisition of selective properties in reactions with organic compounds. Flavonoids are of particular interest, which are the most numerous class of natural phenolic compounds, characterized by structural diversity, high chemical activity and low toxicity. They have a wide range of biological activity, which is associated with many structures that lead to changes in the physicochemical properties of systems based on them [10,11].

Synthesis and use of organic reagents with fluorescent properties in physical-chemical methods of analysis. In recent years, the development of new organic fluorescent reagents, which are further used in various fields of analysis, is becoming more widespread. Thus, in [12] an organic reagent was obtained through the reaction of selenoic acid with three aromatic orthodiamines. Selenoic acid reacted with 2,3-diaminonaphthalene in an acidic solution to form 4,5-benzopiaselenol, which has fluorescent properties. It was found that this compound can then be extracted from the acidic phase with organic solvents and used to determine selenium with a detection limit of 0.002 μg. 2,3-diaminonaphthalene has been found to be significantly more sensitive than the previously recommended 3,3'-diaminobenzidine as a fluorescent reagent.

In [13], new bipyridyl receptors for ruthenium (II) imidazole were synthesized, which can recognize anions of chloride, bromide, dihydrogen phosphate, and ATP in mixed polar aqueous-organic solutions by fluorescence. Interestingly, the combined amidimidazole receptor Ruthenium (II) exhibits selectivity for the determination of anhydrous chloride in a solution of acetonitrile – water with a ratio of 90:10. Also, this receptor is selective for the determination of ATP in the acetonitrile – water (50:50) solvent. The aim of [14] was to develop a new fluorescent labeling reagent 9-anthryldiazomethane (ADAM), for carboxylic acids. 9-anthraldehyde hydrazone was first oxidized with N-chlorosuccinimide in an organic solvent such as ethyl acetate to obtain 9-anthryldiazomethane and then used directly as a reagent for the derivatization of carboxylic acids. Both the oxidation reaction and the derivatization reaction were performed at room temperature, and an aliquot of the derivative mixture was introduced directly into the chromatograph. Derivatives of 9-anthrylmethyl esters formed from ADAM and various carboxylic acids were separated on a reversed-phase column by fluorometric detection. This method can be used for the high performance liquid chromatographic determination of long and short chains of fatty acids, keto acids and hydroxy acids.

Also, in [15] the use of fluorescent reagents such as 4-bromomethyl-7-acetoxycomarin (Br-Mac) in high performance liquid chromatography is described. It was found that Br-Mac reacts with carboxylic acids to form esters, which are then separated by liquid phase chromatography. Next, the column eluate was mixed with an alkaline solution, where the labeled carboxylic acids were hydrolyzed to fluorescent coumarin derivatives, which were then passed through a fluorimeter. Thus, a fluorescent hydrolyzate equimolar to a carboxylic acid was determined, the fluorophore

of which is common to each carboxylic acid. There are only slight peak differences for different carboxylic acids. It is established that this method can detect low levels of femtomol in carboxylic acids. 6-oxy-(N-succinimyl acetate)-9-(2'-methoxycarbonyl) fluorescein (SAMF) is a new fluorescein-based fluorescent probe that was developed in [16] as a derivatizing reagent for the determination of aliphatic amines. Stable fluorescence intensity was observed at pH 4–9. Derivatization took place at room temperature for 6 minutes. Separation was performed on a C18 column, where SAMF derivatives with eight aliphatic amines were separated after 28 min with a mobile methanol-water phase (57:43) containing 10 mmol/l H_3Cit_3-NaOH buffer (pH 5.0). In fluorescent detection at $\lambda_{ex}/\lambda_{em}$ = 484/516 nm, the detection limit reached 2–320 fmol (signal-to-noise ratio = 3), which is better than the detection limits obtained in other analytical methods for the determination of aliphatic amines (Table 1). The proposed method has been successfully used to determine aliphatic amines in environmental samples and food products such as lake water, red wine, white wine and cheese.

In [17] morin was studied (Fig. 1) and its interaction with organotin compounds (chemical compounds with tin and carbon substitutes), which is accompanied by green fluorescence.

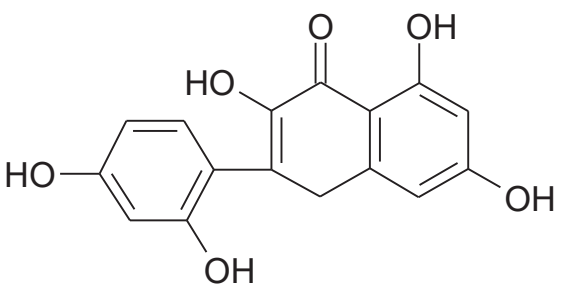

Fig. 1 Structural formula of morin (3,5,7,2',4'-pentahydroxyflavone).

The sensitivity of the reagent for the determination of dialkyltin compounds was especially noted. The excitation and luminescence wavelengths were 415 nm and 495 nm for alkyltin-morin complexes and approximately 405 nm and 520 nm for triphenyltin-morin complexes, respectively. The maximum fluorescence intensity was achieved with the ratio of reagents: from 3 to 9 mol of morin per 1 mol of dialkyl and triphenyltin and from 6 to 12 mol of morin to 1 mol for trialkyltin. The authors set the following limits for the detection of organotin compounds: for dialkyltins $1 \cdot 10^{-9}$ mol/l, for monoalkyltins $1 \cdot 10^{-7}$ mol/l, for trialkyltins $5 \cdot 10^{-7}$ mol/l and $5 \cdot 10^{-7}$ mol/l for triphenyltins (Table 1).

The authors [18] investigated the formation of fluorescent compounds of o-phthaldialdehyde with amino acids in an alkaline medium in the presence of a reducing agent. The excitation and emission wavelengths were 340 nm and 455 nm, respectively. The technique allows to perform fluometric analysis of amino acids to the nanomolar range. It was found that the sensitivity of the method using o-phthaldialdehyde is much higher than that of the method of determination of amino acids by ninhydrin, which was used previously (Table 1).

The phenomenon of fluorescence quenching of rhodamine B due to its interaction with hydroxyl radicals formed by the Fenton reagent was studied in [19]. The inhibitory effect of pentachlorophenol on this interaction has been established. The obtained data allowed the determination of pentachlorophenol with a detection limit of 3.0 ng/ml and a linear range of determination of 4.0–240 ng/ml. The method was used to determine pentachlorophenol in synthetic samples and natural water samples with satisfactory results. A rapid method for

the fluorescence determination of uranium using the interaction between a uranylbenzoic acid complex and Rhodamine B was developed. It was found that the fluorescence intensity depends on the concentration of benzoic acid, the concentration of rhodamine B, pH and the volume of the aqueous phase, and that the increase in fluorescence intensity is proportional to the increase in the concentration of uranium. The detection limit of uranium was $5 \cdot 10^{-8}$ mol/l [20] (Table 1).

A new fluorescent reagent 2-amino-5,7-dimethyl-1,8-naphthyridine was synthesized [21], which was further used to determine trace amounts of nitrites. The authors found that the fluorescence quenching of the reagent by nitrite ion has a linear relationship in the range of nitrite concentrations from $1 \cdot 10^{-7}$ to $2.5 \cdot 10^{-6}$ mol/l with a detection limit of $4.06 \cdot 10^{-8}$ mol/l (Table. 1).

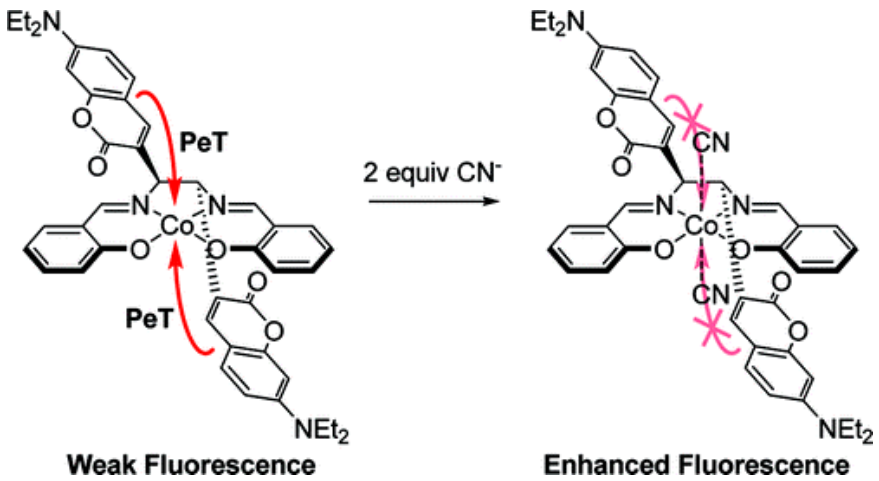

Fig. 2. Enhancement of fluorescent properties in a Co-salen complex in the presence of cyanide ions [22].

A sensor based on a Co (II) complex [22] was developed to determine cyanide anions, which are able to form a 1:2 complex in comparison with other anions. The complex was synthesized by adding 2,2-dihydroxyphenyl ethylenediamine to two equivalents of 7-di-ethylaminocoumarin-3-carboxaldehyde. The resulting compound was then mixed with cobalt (II) acetate in the presence of triethylamine (TEA) followed by recrystallization of the complex in methanol and dichloromethane. With increasing cyanide concentration, the authors observed an increase in the fluorescence intensity of the complex due to the cessation of the process of photoinduced electron transfer from coumarin fluorophore to cobalt (II) ion (Fig. 2).

Analysis of literature shows that increasing the fluorescent properties of complexes in the presence of anions is possible by stopping the process of photoinduced electron transfer from the organic fluorophore to metal ion, and that determination of organotin compounds is possible using complexes with morin. Other complexing agents are ineffective.

Table 1

Detection limits and linear ranges of fluometric methods using organic reagents.

Organic reagent	Analytes	Determination limit	Linear range of concentration change	Reference
2,3-diaminonaphtalene	Selenium	0,002 мкг	–	[12]
(3,5,7,2',4'- pentahydroxyflavone) Morin	Organotin compounds	$1{\cdot}10^{-7}$ - $1{\cdot}10^{-9}$ mol/l	–	[16]
6-oxy-(N- succinimilacetate)-9-(2'-methoxycarbonyl) fluorescein	Aliphatic amines	2–320 fmol	–	[17]
[9-(2- carboxyphenyl)-6-diethyl-amino-3- xanthenyliden]-diethyl-ammonium cloride) Rhodamine B	Pentachloro-phenol	3,0 ng/ml	4,0-240 ng/ml	[19]
Rhodamine B	Uranium	$5{\cdot}10^{-8}$ mol/l	–	[20]
2-amino-5,7-dimethyl-1,8-naphthyridine	Nitrites	$4{,}06{\cdot}10^{-8}$ mol/l	$1{\cdot}10^{-7}$ - $5{\cdot}10^{-6}$ mol/l	[21]

Approaches to detecting the content of metals and proteins using the fluorescent properties of morin complex compounds. Flavonoids are most often used in modern methods of analysis to determine metals. Morin, which belongs to this class of compounds (Fig. 1), can form stable complexes with metal cations, which in some cases have fluorescent properties in the presence of protein structures in solutions. Also, these complexes are quite stable when interacting with protein molecules in a wide pH range (table 2). In [23], the interaction of a Bi (III)-morin complex with DNA using methyl blue dye was studied using fluorescence, spectrophotometry and voltammetry. A Bi (III)-morin (2:1) complex was used in the work, the composition of which was calculated from the results of UV-Vis spectroscopy. It was found experimentally that the fluorescence signal of the Bi (III)-morin complex increases with the addition of DNA, while the fluorescence signal of pure morin decreases accordingly. Addition of methyl blue to the Bi (III)–morin–DNA complex reduces the emission signal and causes a hypochromic shift of 2 nm, which confirms the intercalation of the complex into the DNA molecule. The stability constant of the Bi (III)–morine complex with DNA, which is $2{,}8{\cdot}10^4$, was found in the work.

Table 2

Stability constants of metal complexes with morin [24].

Metal ion	Stability constant, *logβ*	pH
Cu (II)	4,94	5,8
Zn (II)	6,74	5,5
WO_4^{2-}	11,6	3,0
Pd(II)	4,55	4,0
$Ti(C_2O_4)_2^{2-}$	7,35	8,0
Ba (II)	4,55	4,2

During extraction into isopropyl alcohol from acid solutions at different pH values, the duration of fluorescence of morin complexes was established [25]. Complexes of Al (III), Ga (III) and In (III) change their composition in accordance with the change in the acidity of the medium and form complexes with molar ratios of 1:1 or 1:2 (metal:morin). The lifetime of fluorescence or the average lifetime of the molecule in the excited state also changed according to the change in the composition of the complex. Such properties have made it possible to develop optical sensors for detecting ions of these metals. The sensor was based on the formation of a complex between specific metal ions and the complexing ligand. Several chelate systems and several mechanisms of their immobilization are proposed. Morin and its complexes with AI^{3+}, Ga^{3+} and In^{3+} at a concentration of 5 μmol are markedly fluorescent when exposed to normal indoor lighting. Morin complexes with AI^{3+}, Ga^{3+} and In^{3+} were excited at a wavelength of 457.9 nm, the emission wavelength was 525 nm. These spectra overlap strongly, and therefore morin complexes are difficult or impossible to distinguish by conventional fluometric methods. Immobilization did not lead to significant changes in the duration of luminescence of metal-morin complexes. Thus, the sensor based on morin and the formation of its complexes with AI^{3+}, Ga^{3+} and In^{3+} was not suitable for multi-element determinations using spectrofluorometry [26].

The aim of [27] was to determine Aluminum using three different methods based on an Al (III)-morin complex. The methods of spectrophotometry, spectrofluorometry and differential pulse adsorption stripping voltammetry were compared under optimized experimental conditions. Fluorescence spectra were measured in acetoacetate at pH = 5, the concentration of morin was 10 μmol. The maximum excitation wavelength was set to λ_{ex} = 350 nm, and the emmition spectra were recorded in the range from 400 to 650 nm. The maximum fluorescence intensity was reached at λ_{em} = 505 nm. The authors found that the emission intensity is influenced by many factors, including the acidity of the solutions and the concentration of morin. A calibration graph for the determination of Al (III) from 0.1 to 1.0 μmol was also obtained. The method showed good reproducibility and a detection limit of 110 nmol.

In [28], complexes of Al (III) with morin and quercetin were studied by fluorescence. The stoichiometry of the complexes was evaluated by the Job method, the number of fluorescent forms in the solution was calculated by the TRES method. It was found that Al (III) with morin is able to form two complexes with stoichiometries of morin:Al (III) either 1:1 or 2:1 with lifetimes of 4.3 and 2.0 ns, respectively. Morin, which was immobilized on cellulose powder and attached to the end of bifurcated optical fiber, was used to determine Al^{3+} based on their fluorescent complex [29]. When immobilized morin was placed in a solution containing Al^{3+}, the authors observed the fluorescence of the Al (III)-morin complex. A linear dependence of the fluorescence intensity on the wavelength in the range of Al (III) concentrations from $1{\cdot}10^{-6}$ to $1{\cdot}10^{-4}$ mol/l with the detection limit of $1{\cdot}10^{-6}$ mol/l was established. The study of the effect of pH on the fluorescence of the complex showed that at a low acidity of solutions, the stability constant of the complex decreases due to the destruction of the complex due to Al^{3+} protonation, and that at high pH, most of aluminum is in the form of hydroxides. Based on this, the most optimal

pH value of 4.8 was established, at which all measurements were performed. The stability constant of the Al (III)–immobilized morin complex of $1.7 \cdot 10^4$ was determined.

The fluorescent activity of the Lanthanum (III)–quercetin–nucleic acid ternary complex was established in [30]. The authors chose natural calf thymus DNA and thermally denatured yeast DNA and RNA as nucleic acids. The fluorescence intensity of the complexes increased with the formation of ternary complexes in the pH range of 7.8-8.3, NH_3 - NH_4Cl was used as a buffer mixture. The maximum fluorescence intensity of the ternary complexes was observed at an emission wavelength of 470 nm and at an excitation wavelength of 280 nm. Based on these observations, a technique for the determination of nucleic acids was developed. The concentrations of La (III) ($2.2 \cdot 10^{-5}$ mol/l) and quercetin ($5.0 \cdot 10^{-5}$ mol/l) were selected to establish the optimal conditions. The authors obtained calibration graphs with linear ranges of 0.5-3.0 μg/ml for calf thymus DNA and 0.5-4.0 μg/ml for yeast DNA and RNA. The limits of detection were calculated by the 3σ test and were 0.072 μg/ml, 0.142 μg/ml and 0.307 μg/ml for calf thymus DNA, yeast DNA and RNA, respectively.

It is also possible to determine the content of nitric oxide in aqueous and methanolic solutions based on fluorescence using a copper complex with tridentate N-donor ligand, in which with increasing amount of nitric oxide there is an increase in the fluorescence intensity of copper with fluorescent ligand in degassed methanol and aqueous solution (pH=7.2) [31]. Thus, this complex can function as a sensor of nitric oxide based on fluorescence. It is noteworthy that it is possible to determine nanomolar amounts of nitric oxide.

The effect of room temperature ionic liquid on the formation of the fluorescent ternary oxalate-sodium morine-5-Aluminum sulfonate complex was studied [32]. In the presence of 1-butyl-3-methylimidazole hexafluorophosphate (BMIM-PF6) the formation of a complex with better fluorescent characteristics is achieved and as a result a sensitive method for the determination of oxalate ions has been developed. The maximum excitation wavelength was set λ_{ex} = 420 nm, and emission λ_{em} = 513 nm. The detection limit of oxalate is 0.57 ng/ml. The method showed satisfactory results in determining the content of oxalate in plant tissue (spinach leaves).

Using the effects of amplification and quenching of fluorescence to determine organic compounds and metal ions. In [33], the enhancement of fluorescence of a Eu^{3+} tetracycline complex due to DNA or RNA was studied. It was found that double-stranded and single-stranded DNA can strongly enhance the fluorescence of the Eu^{3+} tetracycline complex, in contrast to RNA, which showed a very small amplification effect, based on which a method of selective determination of DNA in the presence of RNA was developed. The most optimal pH conditions, when the maximum fluorescence intensity was reached at an acidity of solutions of 8.0–9.7. The excitation wavelength at which the complex was excited was 398 nm, and the fluorescence wavelength was 615 nm. Calibration graphs with linearity ranging from 0.02 to 1.0 μg for single-stranded and double-stranded DNA were obtained. The relative standard deviation (at n = 7) was in the range of 3.0%.

In [34], a new spectrofluometric method for the determination of lysozyme in the formation of its triple complex with Eu^{3+}-metacycline was developed. Due to the intramolecular

energy transfer from the ligands to the central Eu^{3+} atom, the fluorescence intensity increases threefold at an emission wavelength of 612 nm. The excitation wavelength is 285 nm. Optimal conditions were also established: pH 9.6, metacycline concentration $2.0 \cdot 10^{-5}$ mol/l and Eu^{3+} concentration $2.4 \cdot 10^{-5}$ mol/l The increase in fluorescence intensity is proportional to the lyozyme concentration, the linear range is from 0 to $3.5 \cdot 10^{-5}$ mol/l with a detection limit of $4.74 \cdot 10^{-7}$ mol/l. The mechanism by which an increase in fluorescence between the Eu^{3+} metacycline complex and lysozyme occurred was also investigated. The developed method is simple, sensitive and has been successfully used to determine lysozyme in urine.

In [35], another approach was used to determine cysteine and glutathione with quenching of the fluorescence of the complex. It was found that the addition of thiol compounds to the fluorescent system Zn (II)-8-hydroxyquinoline-5-sulfonic acid Zn (II)-HQS in a buffer mixture of H_3BO_3-$Na_2B_4O_7$ (pH 8.50) leads to quenching of the fluorescence of the complex. Based on these studies, a linear dependency was obtained between the amount of cysteine or glutathione and the corresponding decrease in the relative fluorescence intensity of the Zn (II)-HQS system. The complexes were excited at a wavelength of 365 nm, and the emission wavelength was 512 nm. For optimal conditions, HQS and Zn (II) concentrations of $4.44 \cdot 10^{-6}$ mol/l and $4.59 \cdot 10^{-6}$ mol/l were taken. In the analysis of cysteine in the protein hydrolyzate and reduced glutathione in blood serum, the detection limits were 17 ng/ml and 0.6 μg/ml, respectively. The removal degree was 95.6-104.5%.

The effect of protein on the fluorescence of zinc complexes with morin and fluorescein was studied [36]. The introduction of protein into the Zn-morin complex causes the quenching of fluorescence, which is proportional to the amount of protein. Under optimal conditions, the limits of detection for the determination of bovine serum albumin and human serum albumin are 0.22 g/ml and 0.18 g/ml, respectively.

Based on the fluorescence of DNA-platinum complexes, new methods for the determination of platinum have been developed [37]. The authors found that cis- or trans-bidentate complexes are formed between DNA and platinum. DNA with ethidium bromide forms fluorescent complexes, and the addition of platinum inhibits the intercalation of ethidium bromide, and as a result there is a linear decrease in fluorescence intensity. The method was tested in different ionic media and in a wide range of ionic strength. The detection limit of platinum is $5 \cdot 10^{-8}$ g/ml.

The aim of the study [38] was to develop a sensor for mercury ions based on the fluorescence of iodide anion with the complex T-Hg^{II}-T (T = thymine). The authors synthesized a fluorescent anthracene-thymine (An-T) dyad, which forms with the Mercury ion an An-T-Hg^{II}-T-An complex, and it was found that the addition of mercury reduces the fluorescence intensity. In this case, the dyad A-T is a sensor for mercury (II) ions in aqueous media based on fluorescence quenching. However, with the addition of iodide, the fluorescence of the An-T-Hg^{II}-T-An complex is restored due to the binding of mercury to the iodide ion. The detection limit for iodine is 126 nmol. The sensor has shown high selectivity over other common anions and can be used to detect iodide in drinking water and biological fluids such as urine.

Influence of surfactants on the fluorescence intensity of complexes with morin. The use of micellar systems in spectrophotometric methods of analysis is the most popular and oldest field of application of surfactants in analytical chemistry. In recent years, surfactants have been successfully used in fluorometric determinations. In many cases, there is a multiple increase in fluorescence intensity, which leads to increased interest in these systems due to high sensitivity and selectivity.

In [39] the effect of cationic surfactants on the fluorescence of the zirconium (IV)-morine system is described. It was found that in a sulfuric acid medium the fluorescence intensity of this complex can be greatly enhanced by the cationic surfactant cetyltrimethylammonium bromide (CTAB). However, the addition of a nonionic surfactant TritonX-100 only slightly enhanced fluorescence, and the introduction of anionic surfactants such as sodium lauryl sulfate (SLS) and sodium dodecyl sulfonate (SDS) did not increase the fluorescence intensity. It was found that the determinant factor is the change of the composition of the analyzed complex in the presence of CTAB. When the concentration of CTAB reaches the critical concentration of micelle formation, a complex is formed with the ratio Zr (IV):morin = 1:3. As the concentration of CTAB increases, a mixed complex with the composition Zr (IV): morin:SO_4^{2-} = 1:1:2 is formed, and the fluorescence intensity sharply increases. It was found that the formation of mixed-ligand complexes of zirconium with several anions in the presence of cationic surfactants increase the fluorescence intensity of the system.

The effect of different surfactants on the systems Hf-quercetin, Zr-quercetin, Sn-morin, Mg-oxine-5-sulfonic acid (HIQS), Zn-HzQS, Cd-HZQS and Tb-EDTA-sulfosalicylic acid (SSA) was studied in [40]. Increase in fluorescence occurs due to the formation of complexes such as ionic associates with a rigid structure, which leads to a significant increase in fluorescence intensity. Not only traditional nonionic and cationic surfactants were used, but also zwitterionic and anionic one. It is established that the fluorescence intensity of each investigated complex strongly increases in the presence of the corresponding surfactant. The authors also determined the optimal conditions for the formation of ternary complexes, their structure and quantum yield. It was found that the fluorescence intensity of the complexes changes little when surfactants are added at concentrations lower than the critical micelle concentration (CMC). With a further increase in the surfactant content, the fluorescence intensity begins to increase sharply. Thus, the addition of anionic sodium dodecyl sulfonate (SDS) to the Sn-morin complex increases the fluorescent properties of the system by a factor of 4, and a ternary complex with Sn:morin:SDS = 1:2:2. stoichiometry is formed.

In [41], a simple and sensitive spectrofluorimetric method for the determination of Al (III) based on the formation of the ternary complex Al (III) - morin - Triton X-100 is described. The effects of other nonionic surfactants, such as Tween 80, Tween 20 and octyl glucoside (OG), have also been studied. The addition of Triton X-100 increases the sensitivity fivefold in the fluorometric determination of Al (III) using morin. The complex was excited at a wavelength of 410 nm, and the fluorescence signal was measured at a wavelength of 495 nm. The maximum fluorescence signal was observed at pH 4.0 (acetate buffer), with 0.6% TX-100 and at a morin concentration of $1.35 \cdot 10^{-3}$ mol/l. The

authors also obtained a calibration graph that is linear up to 7 mg/l, and the detection limit is 0.022 mg/l. The use of Triton X-100 eliminates the need to use additional extraction steps for the sensitive and selective determination of Al (III).

The effect of the anionic surfactant sodium dodecylbenzenesulfonate (SDBS) on the fluorescence intensity of the Al (III) – morin complex and the mechanism of their interaction were studied in [42]. It was found that the luminescence increases and, on this basis, a fluometric method for the determination of proteins was developed. The highest fluorescence intensity was achieved at pH 6.84, and it was also shown that the fluorescence intensity is influenced by the type of buffer mixture, among which the most effective was HMTA – HCl. The maximum fluorescence intensity was reached at concentrations of morin and Al (III) of $1.0 \cdot 10^{-6}$ mol/l and $1.0 \cdot 10^{-5}$ mol/l, respectively. Regarding the anionic surfactant SDBS, its concentration was $2.0 \cdot 10^{-4}$ mol/l, which is lower than the critical micelle concentration, which is $3.3 \cdot 10^{-4}$ mol/l for SDBS. Under optimal conditions, the increased fluorescence intensity was proportional to the protein concentration in the range of $1.0 \cdot 10^{-8}$–$1.3 \cdot 10^{-5}$ g/ml for bovine serum albumin (BSA), $4.0 \cdot 10^{-8}$–$1{,}2 \cdot 10^{-5}$ g/ml for egg albumin (EA) and $5.0 \cdot 10^{-8}$–$1.2 \cdot 10^{-5}$ g/ml for human serum albumin (HSA). The limits of their detection were $5.0 \cdot 10^{-9}$, $1.8 \cdot 10^{-8}$ and $1.6 \cdot 10^{-8}$ g/ml, respectively. Thus, the authors obtained a highly sensitive, stable and rapid method for the determination of proteins.

An increased fluorescence intensity of the aluminum (III)-morin complex was observed in [43] in the presence of the nonionic surfactant Tween-20. The fluorescence of the complex was measured at an excitation wavelength of 425 nm and an emission wavelength of 495 nm. The authors also established optimal conditions: pH = 4.5, the concentration of morin 20 mmol, and 0.8% Tween-20. A linear calibration graph from 50 to 100 μg/l was also obtained, and the detection limit was 3 μg/l.

In [44], a highly sensitive method of fluorometric determination of Fe (III) by reaction with 5-(4-methoxyphenylazo)-8-(4-toluenesulfonamido) quinoline in the presence of the cationic surfactant cetyltrimethylammonium bromide (CTAB) is described. As a result, a linear fluorescence intensity (λ_{ex} = 317 nm, λ_{em} = 534 nm) of up to 3 mmol (170 ng/ml) of Iron (III) in an aqueous solution was observed. A similar experiment was also performed in the presence of the anionic surfactant sodium dodecyl sulfate. The introduction of anionic surfactants led to a decrease in fluorescence intensity. In contrast to this, the introduction of the nonionic surfactants Tween-80 and TritonX-100 into the studied system as well as cationic surfactants (CTAB) increased the fluorescence intensity but gave larger background signals. The most optimal concentration of CTAB was determined, which was $1.7 \cdot 10^{-3}$ mol/l, which is higher than the critical concentration of micelle formation (CMC (CTAB) = $1.3 \cdot 10^{-3}$ mol/l). This method can also be used to determine the trace amounts of Fe (III) and Fe (II) without the need for prior concentration.

In [45], the authors determined how the addition of nonionic surfactants affects the fluorescence intensity of Al (III)-morin complexes in order to improve the analytical characteristics of the complex. Morin is one of the reagents most often used for the qualitative and quantitative determination of Al (III). The authors found that the addition of cationic surfactants such as cetyltrimethylammonium

bromide (CTAB) and nonionic surfactants such as: polyoxyethylene noniphenols, polyoxyethylene higher alcohols, fatty carboxylic acid esters and alkanolamides do not increase the fluorescence intensity, but on the contrary, cause its significant decrease contrary to the expectations of the authors. Only in some cases there were an initial increase in luminescence intensity at high surfactant concentrations and subsequent quenching with increasing content of nonionic surfactant in the system. In contrast, the authors found that the addition of GenapolPF-20 (ethylene oxide – condensate of epoxypropane) to the metal-morin complex causes an increase in fluorescence intensity, so the sensitivity of the determination can be increased tenfold, as well as the selectivity of the method compared to other methods. The optimal conditions for increasing the fluorescence intensity were: the concentration of nonionic surfactant 3%, morin 0.005%, pH 3.8 in an acetate buffer at a temperature of 25 °C. The excitation and emission wavelength maxima were λ_{ex} = 430 nm and λ_{em} = 495 nm, respectively. The maximum fluorescence intensity was observed after 1.5 hours and remained stable for another 5 hours, the detection limit was 0.2 μg/l. The introduction of surfactants did not lead to either bathochromic or hypsochromic shift, which indicates a slight effect of surfactants on the ground and excited states of the complex. It was also shown that other derivatives of polyoxyethyl compounds resulted in increased sensitivity in the same order, but with a different surfactant concentration.

In [46], the fluorometric determination of samarium and gadolinium by increasing the fluorescence of the samarium-tenoyltrifluoroacetone-gadolinium 1,10-phenanthrolinate complex (Sm (III) – TTA – Phen – Gd (III)) was investigated, which increases the fluorescence intensity almost twofold. To increase the stability of the Sm (III) – TTA – Phen – Gd (III) system, surfactants were added, and their effects were investigated. Thus, the cationic surfactant CTAB and nonionic surfactant Tween-80 caused a decrease in fluorescence intensity. In contrast, the nonionic surfactants TX-100 and PVA caused a sharp increase in the fluorescence intensity of the complex.

Therefore, TX-100 was used for further experiments. An increase in the fluorescence intensity at the concentration of TX-100 at the level of the critical micelle concentration was shown. The most optimal concentration range of TX-100 was 0.018–0.064% (fivefold increase in emissions). A further increase in the concentration of TX-100 led to a decrease in emission intensity. It is noteworthy that the excess of TX-100 caused a bathochromic shift of the maximum excitation wavelength. The maximum fluorescence intensity was obtained in a pH range of 5.3–6.0 at a wavelength of excitation and emission of 349 nm and 648 nm, respectively. Thus, the system Sm (III) – TTA – Phen – Gd (III) – TritonX-100 can be used to determine trace amounts of samarium in lanthanide oxides.

The aim of [47] was to determine tetracyclines (TC) in aqueous solutions based on the formation of fluorescent chelates with europium using EDTA as a coligand and cetyltrimethylammonium chloride (CTAC) as a surfactant. The method involves the formation of a chelate, where the lanthanide ion will be associated with the β-diketone group. Contrary to the authors' expectations, the addition of the nonionic surfactant TX-100 almost does not change the luminescence intensity in the pH range 5-9, and the addition

of EDTA has a negative effect and sharply reduces the fluorescence intensity. At the same time, with the addition of CTAC, the emission intensity increased and reached a maximum at pH 9. The Eu – TC – CTAC system has a sensitivity that is 6 times higher than that of the Eu – TC – TX-100 system, and the detection limits were $2{,}5\cdot10^{-10}$, $5\cdot10^{-10}$, $1{,}5\cdot10^{-9}$ and $2\cdot10^{-9}$ mol/l for TC, oxytetracycline, chlortetracycline and doxycycline, respectively.

In [48], the authors found how the molecular structure of the anionic surfactant affects the fluorescence of bovine serum albumin (BSA). Sodium alkyl sulfates (C_nSO_3, n = 8, 10, and 12) and sodium alkyl carboxylates (C_nCOONa, n = 9 and 11) were used as anionic surfactants. It was established that with the increase of the hydrophobic chain the ability to quench the fluorescence of BSA increases, and the hypsochromic shift increases. It is noteworthy that the replacement of acidic groups of anionic surfactants does not show a significant effect on the fluorescence of the albumin complex.

The authors of [49] studied the effect of surfactants on the fluorescence of the beryllium-morin system. It was found that the addition of the nonionic surfactant TX-100 significantly increases the fluorescence intensity of the complex, as opposed to the anionic surfactant sodium lauryl sulfate (SLS), zwitterionic surfactant dodecyldimethylaminoacetic acid (DDMAA), and cationic surfactant cetyltrimethylammonium bromide (CTAB), which cause only a slight increase of fluorescence. It was also found that when adding all surfactants, except for anionic SLS, a bathochromic shift occurs (up to 25 nm). The addition of Triton X-100 makes it possible to determine the nanoquantities of beryllium in weakly acidic solutions (pH 5.8–6.2, hexamine buffer solution), detection limit 0.06 ng/ml. The relative standard deviation is 2.2% for beryllium at a concentration of 0.5 ng/ml and 0.7% for 5.0 ng/ml. The method is used to determine beryllium in water quality control samples and therefore the effect of 25 ions that can affect the fluorescence of the Be-morin-TX-100 complex, among which Zn^{2+} and F^- interfere the most, was also studied.

In [50], a method of determination of Al (III) in a luminescent complex with lumogallion is presented. The addition of the nonionic surfactant Triton X-100 increased the fluorescence intensity of the Al (III)-morin complex by a factor of 5–6. Optimal conditions were also determined: pH 4.7, the concentrations of lumogallion and TX-100 were 1 μg/l and 0.5%, respectively. The detection limit of Al (III) is 0.2 μg/l. The sensitivity of the method does not depend on the salt concentration in water and can be used to determine aluminum in water.

Therefore, to date, the study of the effect of surfactants on the fluorescent properties of organic reagents and their complexes continues, because the increase or decrease in fluorescent properties is not systematic and is not always explainable.

CONCLUSIONS. To date, the complexes of morin with metals are actively studied and tend to be widely used in such physicochemical methods of analysis as: high performance liquid chromatography, spectrophotometry and fluorometry. It has been proved that in complex compounds of cobalt and salen, the increase of the fluorescent properties of complexes in the presence of anions is possible by stopping the process of photoinduced electron transfer from organic fluorophore to metal ion, and the determination of organotin

compounds is possible using complexes with morin. Other complexing agents are less effective and ineffective. The most studied is the complex Al (III) - morin in comparison with complexes of morin with other metals, such as In (III), Bi (III) and Ga (III). These complexes can be used to determine metals or to detect DNA of different biological origin or for the quantitative analysis of protein. All complexes with morin are stable in a wide pH range (3-8) and have a high fluorescence intensity. The fluorescence intensity can be increased by adding surfactants. For protein systems of morin with some metals (zinc and mercury), an opposite phenomenon is observed – fluorescence quenching, which can be used for the quantitative determination of proteins and metals.

ACKNOWLEDGMENT.
The work was done under financial support of Ministry of Education and Science of Ukraine.

В огляді описано сучасні фізико-хімічні системи на основі комплексних сполук з органічними лігандами, які можуть мати флуоресцентні властивості при взаємодії з іонами металів або білками. Наведено сучасні методи синтезу цих сполук та використання їх у фізико-хімічних методах аналізу. Розглянуто підходи до визначення вмісту металів і білків за флуоресцентними властивостями комплексних сполук морину. Описано сфери використання ефектів ампліфікації та гасіння флуоресценції для визначення органічних сполук та іонів металів, особливо за наявності ДНК та РНК різного біологічного походження. Окремо проаналізовано вплив поверхнево-активних речовин на інтенсивність флуоресценції комплексів із морином.

Ключові слова: морін, комплексні сполуки, флуоресценція, аналіз, іони металів, білок.

МЕТОДИ СИНТЕЗУ ТА ОСОБЛИВОСТІ ВИКОРИСТАННЯ СИСТЕМ НА ОСНОВІ МЕТАЛОКОМПЛЕКСІВ МОРІН У МЕТОДАХ ФЛУОРЕСЦЕНТНОГО АНАЛІЗУ

Асєєва Д. А.[1,2]

[1]*Університет Тулуза III - Поль Сабатьє, 118 траса Нарбон, Тулуза Cedex, 9, 31062, Франція*
[2]*Київський національний університет імені Тараса Шевченка, вул. Володимирська, 60, м. Київ 01033, Україна*
email: dasha.aseeva@gmail.com

REFERENCES

1. Rettig W., Strehmel B., Schrader S., & Seifert H. (Eds.). *Applied fluorescence in chemistry, biology and medicine*. Springer Science & Business Media. 2012.
2. Kulmyrzaev A. A., Karoui R., De Baerdemaeker J., & Dufour E. Infrared and fluorescence spectroscopic techniques for the determination of nutritional constituents in foods. *International Journal of Food Properties*. 2007. **10** (2): 299–320.
3. Kato A., & Nakai S. Hydrophobicity determined by a fluorescence probe method and its correlation with surface properties of proteins. *Biochimica et biophysica acta (BBA)-Protein structure*. 1980. **624**(1): 13–20.

4. Jin H. G. Z. X. O. Application of Chemiluminescent Image to Biological Molecules Detection. *World Sci-tech R & D*, 04. 2004.
5. Paramita V. D., & Kasapis S. The role of structural relaxation in governing the mobility of linoleic acid in condensed whey protein matrices. *Food Hydrocolloids*. 2018. **76**. 184–193.
6. Tran T. M., Dai T. X. T., Tran D. B., Nguyen Q. C. T., & Nguyen D. H. Y. A simple spectrophotometric method for quantifying total lipids in plants and animals. *Can Tho University Journal of Science*. 2019. **11**(2): 106–110.
7. Gazioglu I., Zengin O. S., Tartaglia A., Locatelli M., Furton K. G., & Kabir A. Determination of polycyclic aromatic hydrocarbons in nutritional supplements by fabric phase sorptive extraction (FPSE) with high-performance liquid chromatography (HPLC) with fluorescence detection. *Analytical Letters*. 2020. **54**(10): 1683–1696.
8. Abd Ali L. I., Qader A. F., Salih M. I., & Aboul-Enein H. Y. Sensitive spectrofluorometric method for the determination of ascorbic acid in pharmaceutical nutritional supplements using acriflavine as a fluorescence reagent. *Luminescence*. 2019. **34**(2): 168–174.
9. Muñoz-Huerta R. F., Guevara-Gonzalez R. G., Contreras-Medina L. M., Torres-Pacheco I., Prado-Olivarez J., & Ocampo-Velazquez R. V. A review of methods for sensing the nitrogen status in plants: advantages, disadvantages and recent advances. *Sensors*. 2013. **13**(8): 10823–10843.
10. Panche A. N., Diwan A. D., & Chandra S. R. Flavonoids: an overview. *Journal of nutritional science*, *5*. 2016.
11. Harborne J. B., Marby H., & Marby T. J. *The flavonoids*. Springer. 2013.
12. Parker C. A., & Harvey L. G. Luminescence of some piazselenols. A new fluorimetric reagent for selenium. *Analyst*. 1962. **87**(1036): 558–565.
13. Vickers M. S., Martindale K. S., & Beer P. D. Imidazolium functionalised acyclic ruthenium (II) bipyridyl receptors for anion recognition and luminescent sensing. *Journal of Materials Chemistry*. 2005. **15**(27–28): 2784–2790.
14. Yoshida T., Uetake A., Yamaguchi H., Nimura N., & Kinoshita T. New preparation method for 9-anthryldiazomethane (ADAM) as a fluorescent labeling reagent for fatty acids and derivatives. *Analytical biochemistry*. 1988. **173**(1): 70–74.
15. Tsuchiya H., Hayashi T., Naruse H., & Takagi N. High-performance liquid chromatography of carboxylic acids using 4-bromomethyl-7-acetoxycoumarin as fluorescence reagent. *Journal of Chromatography A*. 1982. **234**(1): 121–130.
16. Arakawa Y., Wada O., & Manabe M. Extraction and fluorometric determination of organotin compounds with Morin. *Analytical Chemistry*. 1983. **55**(12): 1901–1904.
17. .Cao L. W., Wang H., Li J. S., & Zhang H. S. 6-Oxy-(N-succinimidyl acetate)-9-(2'-methoxycarbonyl) fluorescein as a new fluorescent labeling reagent for aliphatic amines in environmental and food samples using high-performance liquid chromatography. *Journal of Chromatography A*. 2005. **1063**(1-2): 143–151.
18. Roth M. Fluorescence reaction for amino acids. *Analytical Chemistry*. 1971. **43**(7): 880–882.
19. Fan J., Guo H. Q., & Feng S. L. Spectrofluorimetric determination of pentachlorophenol based on its inhibitory effect on the redox reaction between hydroxyl radicals and fluorescent dye rhodamine B. 2007.
20. Andersen N. R., & Hercules D. M. Fluorometric Determination of Uranium with Rhodamine B. *Analytical Chemistry*. 1964. **36**(11): 2138–2141.
21. Chen T., Tong A., & Zhou, Y. 2-Amino-5, 7-dimethyl-1, 8-naphthyridine as a fluorescent reagent for the determination of nitrite. *Spectrochimica Acta Part A: Molecular and Biomolecular Spectroscopy*. 2007. **66**(3): 586–589.
22. Lee J. H., Jeong A. R., Shin I. S., Kim H. J., & Hong J. I. Fluorescence turn-on sensor for cya-

nide based on a cobalt (II) – coumarinylsalen complex. *Organic letters*. 2010. **12**(4): 764–767.
23. Ensafi A. A., Hajian R., & Ebrahimi S. Study on the interaction between morin-Bi (III) complex and DNA with the use of methylene blue dye as a fluorophor probe. *Journal of the Brazilian Chemical Society*. 2009. **20**(2): 266–276.
24. Malešev D., & Kuntić V. Investigation of metal-flavonoid chelates and the determination of flavonoids via metal-flavonoid complexing reactions. *Journal of the Serbian chemical society*. 2007. **72**(10): 921–939.
25. Sawada T., Shibamoto T., & Kamada H. Fluorescence Lifetime Measurements of Morin–Metal Ion Complexes. *Bulletin of the Chemical Society of Japan*. 1978. **51**(6): 1736–1738.
26. Carroll M. K., Bright F. V., & Hieftje G. M. Fiber-optic time-resolved fluorescence sensor for the simultaneous determination of aluminum (3+) and gallium (3+) or indium (3+). *Analytical Chemistry*. 1989. **61**(15): 1768–1772.
27. Domínguez-Renedo O., Navarro-Cuñado A. M., Ventas-Romay E., & Alonso-Lomillo M. A. Determination of aluminium using different techniques based on the Al (III)-morin complex. *Talanta*. 2019. **196**: 131–136.
28. Gutierrez A. C., & Gehlen M. H. Time resolved fluorescence spectroscopy of quercetin and morin complexes with Al^{3+}. *Spectrochimica Acta Part A: Molecular and Biomolecular Spectroscopy*. 2002. **58**(1): 83–89.
29. Saari L. A., & Seitz W. R. Immobilized morin as fluorescence sensor for determination of aluminum (III). *Analytical Chemistry*. 1983. **55**(4): 667–670.
30. Zhou J., Gong G. Q., Zhang Y. N., Qu J. Q., Wang L. F., & Xu J. W. Quercetin–La (III) complex for the fluorimetric determination of nucleic acids. *Analytica chimica acta*. 1999. **381**(1): 17–22.
31. Mondal B., Kumar P., Ghosh P., & Kalita A. Fluorescence-based detection of nitric oxide in aqueous and methanol media using a copper (II) complex. *Chemical Communications*. 2011. **47**(10): 2964–2966.
32. Nizar S. A., & Suah F. B. M. Effect of room temperature ionic liquid on the formation of the complex oxalate-sodium morin-5-sulfonate-aluminium (III): Application to the fluorescence determination of oxalate ion. *Journal of fluorescence*. 2016. **26**(4): 1167–1171.
33. Ci Y. X., Li Y. Z., & Liu X. J. Selective determination of DNA by its enhancement effect on the fluorescence of the Eu3+-tetracycline complex. *Analytical Chemistry*. 1995. **67**(11): 1785–1788.
34. Chongqiu J., & Li L. Lysozyme enhanced europium–metacycline complex fluorescence: a new spectrofluorimetric method for the determination of lysozyme. *Analytica chimica acta*. 2004. **511**(1): 11–16.
35. Wang H., Wang W. S., & Zhang H. S. A spectrofluorimetric method for cysteine and glutathione using the fluorescence system of Zn (II)–8-hydroxyquinoline-5-sulphonic acid complex. *Spectrochimica Acta Part A: Molecular and Biomolecular Spectroscopy*. 2001. **57**(12): 2403–2407.
36. Huang W., Cao N., & Wang F. Determination of Serum Albumin by its quenching effect on the fluorescence of Zn 2-Morin complex. 2016.
37. Butour J. L., & Macquet J. P. Platinum determination in DNA-platinum complexes by fluorescence spectrophotometry. *Analytical biochemistry*. 1978. **89**(1): 22–30.
38. Ma B., Zeng F., Zheng F., & Wu S. A. Fluorescence Turn – on Sensor for Iodide Based on a Thymine – HgII – Thymine Complex. *Chemistry – A European Journal*. 2011. **17**(52): 14844–14850.
39. Fan Y. X., & Zheng Y. X. Effect of cationic micelles on the fluorescence of the zirconium – morin complex. *Analytica chimica acta*. 1993. **281**(2): 353–360.
40. Hui-Ming S., Wan-Cang C., & Ru-Ji W. Sensitization of surfactant on the fluorescent

reactions of metals. *Acta Chimica Sinica English Edition*. 1984. **2**(2): 133–143.
41. Suah F. B. M., Ahmad M., & Mehamod F. S. Effect of non-ionic surfactants to the Al (III)-morin complex and its application in determination of Al (III) ions: A preliminary study [Kesan surfaktan tak-ionik kepada kompleks Al (III)-morin dan aplikasinya dalam penentuan ion Al (III): Satu kajian awal]. *Malaysian Journal of Analytical Sciences*. 2017.
42. Wang F., Yang J., Wu X., Sun C., Liu S., Wang F., & Jia Z. Fluorescence enhancement effect of the morin–Al3+–sodium dodecyl benzene sulphonate – protein system and the determination of proteins. *Luminescence: The journal of biological and chemical luminescence*. 2006. **21**(1): 49–55.
43. Al-Kindy S. M. Z., Suliman F. O., & Salama S. B. A sequential injection method for the determination of aluminum in drinking water using fluorescence enhancement of the aluminum – morin complex in micellar media. *Microchemical journal*. 2003. **74**(2): 173–179.
44. Zeng Z., & Jewsbury R. A. Fluorimetric determination of iron using 5-(4-methoxyphenylazo)-8-(4-toluenesulfonamido) quinoline. *Analyst*. 2000. **125**(9): 1661–1665.
45. Escriche J. M., Cirugeda M. D. L. G., & Hernandez F. H. Increase in the sensitivity of the fluorescent reaction of the complexing of aluminium with morin using surfactant agents. *Analyst*. 1983. **108**(1292): 1386–1391.
46. Ci Y., & Lan Z. Fluorometric determination of samarium and gadolinium by enhancement of fluorescence of samarium-thenoyltrifluoroacetone-1, 10-phenanthroline ternary complex by gadolinium. *Analytical Chemistry*. 1989. **61**(10): 1063–1069.
47. Arnaud N., & Georges J. Sensitive detection of tetracyclines using europium-sensitized fluorescence with EDTA as co-ligand and cetyltrimethylammonium chloride as surfactant. *Analyst*. 2001. **126**(5): 694–697.
48. Lu R. C., Cao A. N., Lai L. H., & Xiao J. X.. Effect of anionic surfactant molecular structure on bovine serum albumin (BSA) fluorescence. *Colloids and Surfaces A: Physicochemical and Engineering Aspects*. 2006. **278**(1–3): 67–73.
49. Wei, F., Ten, E., & Wu, Z.. Enhancement of the fluorescence of the beryllium-morin complex by non-ionic surfactants. *Talanta*. 1990. **37**(9): 947–950.
50. Howard, A. G., Coxhead A. J., Potter I. A., & Watt A. P. Determination of dissolved aluminium by the micelle-enhanced fluorescence of its lumogallion complex. *Analyst*. 1986. **111**(12): 1379–1382.

Стаття надійшла 09.11.2021.

UDC 541.49: 546.562+546.73: 577.164.32 – 54-386 doi: 10.33609/2708-129X.87.10.2021.90-102

SPECTROSCOPIC STUDIES OF Cu (II) AND Co (II) COMPLEXES WITH RUTIN IN SOLUTIONS

O.K. Trunova*, M.S. Artamonov, T.O. Makotryk

V.I. Vernadsky Institute of General and Inorganic Chemistry of the National Academy of Sciences of Ukraine, 32/34 Academic Palladin ave., Kyiv 03142, Ukraine
** e-mail: trelkon@gmail.com*

Complexation in M (II) – Rut systems (M(II) = Co, Cu) was studied by electron absorption spectroscopy and pH-metric titration in water-ethanol solutions depending on the metal: ligand ratio (1: 1; 2: 1) and the pH of the medium. It was shown that the structure and stoichiometric composition of the complexation reaction products are influenced by such basic parameters as L:M and the pH value of the medium. Depending on the pH value, chelation involves certain binding sites, which primarily is associated with the redistribution of the electron density in the flavonoid molecule. In a weakly acidic or neutral medium, regardless of the M(II): Rut ratio, the formation of monoligand complexes of rutin with 3-d metals occurs with the participation of 5-OH and 4-C=O fragments of the A and C rings, and in an alkaline medium, chelation proceeds on the catecholic fragment of ring B rutin. Biligand complexes are formed with the participation of the gydroxo groups of the catechol fragment of each rutin molecule, and the formation of compounds with a ratio of 2:1 occurs both due to 5-OH and 4C=O and due to 3 ', 4'-OH groups. The calculated values of the stability constants of the complexes showed that the stability of the Co (II) complexes is several orders of magnitude lower than the stability of the corresponding Cu (II) complexes.

Keywords: complexes, copper, cobalt, rutin, flavonoids, absorption spectra.

INTRODUCTION. Flavonoids are a large class of natural low-molecular-weight polyphenolic compounds of the general $C_6–C_3–C_6$ carbon skeleton formula, as well as their derivatives, which are characterized by high biological activity and low toxicity. The targeted biological action of flavonoids is related to the physicochemical properties of various structures, including conformations of molecules, the presence of which provides, for example, radioprotective and antioxidant properties. Flavonoids are widely used in plants, in which they play several very important functions, including antioxidant one [1–5]. Rutin (3, 3 ', 4', 5,7-pentahydroxyflavone-3-rhamnoglucoside $C_{27}H_{26}O_{16}H_4$, H_4L, Rut) is a natural flavonoid of the flavonol type, consisting of the flavonol quercetin and the rutinose disaccharide (rhamnose and glucose):

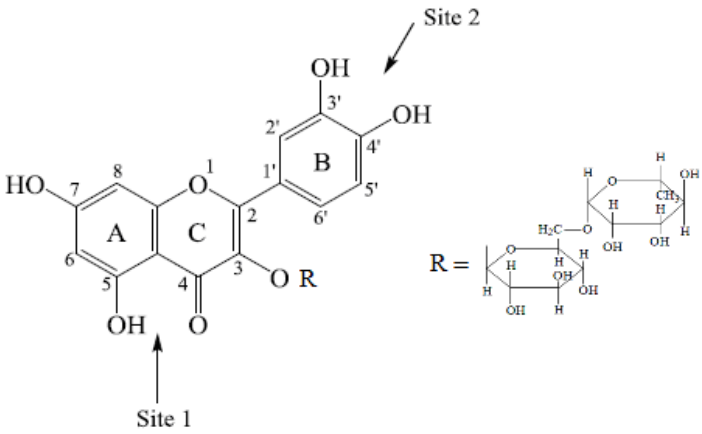

Fig. 1. The structure of the rutin molecule.

It exhibits high biological and pharmacological activity (antioxidant, anti-inflammatory, antiviral, antimicrobial, etc.) [6–12]. Due to its medicinal properties, rutin is widely used as a component of many pharmaceuticals (eg, vitamin P). The most important structural elements of rutin, which determine its properties, are: o-dihydroxo group in the B-cycle (catechol structure) as a potential radical label; the double bond between positions 2 and 3 of the C-cycle is conjugated with the keto group at position 4 (due to the ability to delocalize the unpaired electron of the flavonoid radical) and C-3, C-5 and C-7 hydroxyl groups (C and A cycles) as potential acceptors of free radicals [13,14].

Flavonoids bind metal ions well, forming chelate complexes, which is of great importance for the analytical and pharmaceutical use of these compounds. The formation of different CS structures of flavonoids with metal ions with the stoichiometric composition L: M from 1: 2 to 2: 1 depends on the binding sites that participate in the reaction. As can be seen from the structure of the rutin molecule, in complexes with metals, this flavonoid has two potential centers for coordination to metal ions: 5-OH and 4-C = O, 3'-OH and 4'-OH (Fig. 1). Most metal ions are able to form complexes with rutin in a wide range of pH (2-10), the stereochemistry of which strongly depends on the acidity of the solutions [15-17]. The best complexation occurs at pH 4-8, because at pH<4 rutin is in undissociated form (weak acid), and at pH>8 there is the formation of stoichiometrically different coordination compounds or dissociation of existing complexes. In aqueous solutions, the complexes are poorly soluble, so, as a rule, they are investigated in the form of solid compounds.

Considerable attention in the study of flavonoids is paid to complexes with transition metals, which can be used for the prevention and treatment of many diseases [15, 18,19]. Studies of flavonoids in oxidative processes show that the formation of chelates gives them antioxidant properties, which are more effective in binding free radicals [20–22]. In [20] it was shown that rutin complexes with iron, copper and zinc show increased efficiency in the absorption of free radicals, the most effective of which is the copper complex. The rutin com-

plex with copper has a greater ability to retard the oxidation process, and rutin complexes with iron(II) and copper(II) are more effective in removing free radicals compared to pure rutin [23, 24].

It should be noted that rutin and its complexes due to poor solubility in water and body fluids have a very low bioavailability in the body, which limits the use of their useful pharmacological properties. Increased solubility can be achieved by using other solvents that will also be non-toxic to living organisms. The literature mainly investigates the complexation of rutin with metals in methanol solutions, DMSO or mixtures of different organic solvents [23, 25–28]. Since rutin is poorly soluble in water, but better soluble in ethanol ($0.66 \cdot 10^{-5}$ mol/dm^3 and $436.5 \cdot 10^{-5}$ mol/dm^3, respectively) [1, 29, 30], for the potential application of its useful properties in pharmacology, there is a need to investigate the properties of rutin and its complexes with Cu (II) and Co (II) in aqueous-ethanolic solutions. The choice of metal ions is due to their role in the life of organisms. Copper and cobalt are transition metals and essential trace elements. Cu (II) is part of many vitamins, hormones, enzymes, respiratory pigments, is involved in metabolic processes, tissue respiration and more. Copper ions play an important role of cofactors in living systems, so the presence of competing complexing agents can affect their biological activity [20,31], Co (II) is present in vitamin B12, is involved in enzymatic processes and hormone synthesis [31]. Therefore, the aim of this work is to study the acid-base forms of rutin depending on the pH of the solution and its complexation with Cu(II) and Co(II) in aqueous-ethanol solutions by pH-metric titration and electron absorption spectroscopy.

EXPERIMENT AND DISCUSSION OF THE RESULTS. The study of the complexation of Cu(II) and Co(II) ions with rutin was carried out in water-ethanol solutions (1: 2) depending on pH (~ 2÷11) and the metal:ligand ratio. Inorganic salts of 3-d metals were used as starting compounds: cobalt chloride $CoCl_2 \cdot 6H_2O$ (analytical grade) and copper sulfate $CuSO_4 \cdot 5H_2O$ (analytical grade). Rutin manufactured by Sigma- Aldrich was used without further purification.

The exact concentration of metal ions was determined by complexometric titration [32]. Working solutions of rutin were prepared using a precisely weighed sample. Potentiometric titration was carried out with a 0,1 M solution of alkali (NaOH) or acid (HCl) as a titrant. The pH value was recorded on a Mettler Toledo Seven Easy pH meter (accuracy ± 0.05)at 20 ± 3 °C and constant ionic strength $\mu = 0{,}1$ M (KNO_3). Electronic absorption spectra were recorded on a UV/VIS Specord 210 Plus spectrophotometer (Analytik Jena AG) in quartz cuvettes with l=1 cm (measurement range 190-1100 nm; relative error in the measurement of optical density ±0,005). A series of Co(II) and Cu(II) solutions with rutin was studied at a concentration of $1 \cdot 10^{-4}$ M and the ratio M:Rut = 1:1, 2:1. The comparison solution is water. To establish the stoichiometric composition and stability of the formed complexes, the method of equilibrium displacement was used [33]. Step constants of complex formation were determined by the titration of a solution containing known amounts of C (II) chloride C (II) sulfate and rutin with an acid/alkali solution.

In the electronic absorption spectrum of an aqueous ethanolic solution of rutin (Fig. 2) there are two absorption bands, which are

due to intramolecular π → π * transitions: the first band with a maximum in the area of 327–408 nm corresponds to the absorption of a cynnamoyl fragment of the molecule associated with a conjugated system between cycle B and a carbonyl fragment of cycle C. The second absorption band in the region of 250–290 nm refers to π → π* transitions in the A ring benzoyl fragment [34]

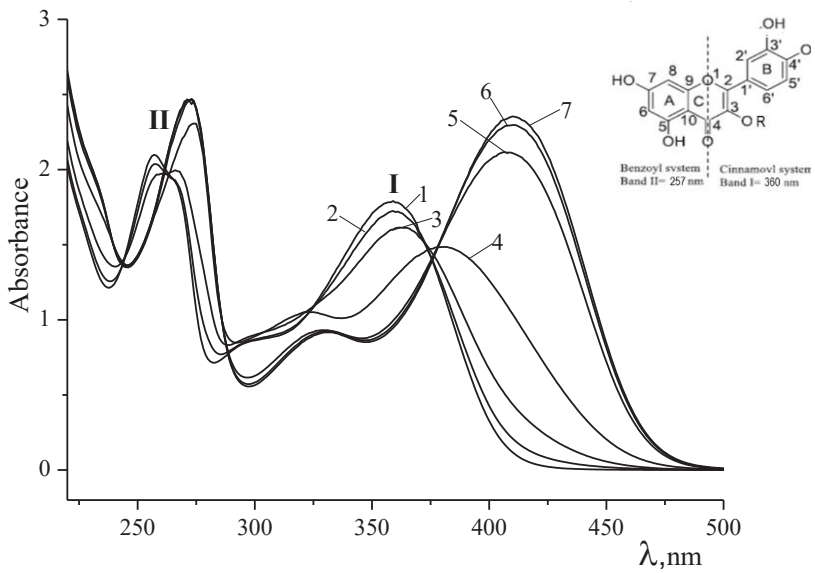

Fig. 2. UV absorption spectrum of an aqueous-ethanol solution of rutin at pH: 1. – 5.6; 2. – 6.3; 3. – 7.0; 4. – 8.2; 5. – 9.7; 6. – 10.4; 7. – 11.4.

The gradual bathochromic shift at pH>6 is associated with the formation of differently protonated forms of rutin, which are in dynamic equilibrium depending on the acidity of the solutions. In the acidic pH range, there is a bathochromic shift of absorption band II with the formation of a shoulder at 290 nm, which disappears at pH~7. At the same time, there is a bathochromic shift of the band I maximum (357 nm→363 nm), which is accompanied by a hypochromic effect. Such changes may be related to the dissociation of the OH group at position 7 of cycle A of the rutin molecule. At pH = 7.74 there are a hypsochromic shift and an increase in the optical density of the solution, which indicates the further dissociation of proton rutin. At pH = 9.65, the optical properties of the system change significantly – two absorption maxima are clearly manifested at λ_{max} = 329 nm and 407 nm. At pH = 11.90, a hypsochromic shift of these absorption maxima is observed, which may be associated with partial oxidation of rutin.

According to spectrophotometric titration, the dissociation constants of rutin and the distribution of acid-base forms of rutin depending on the pH of the solution were calculated using the mathematical program CLINP 2.1 [35] (tab. 1, fig. 3, respectively).

Table 1

Values of rutin dissociation constants in an aqueous ethanol solution.

Dissociation stage	pK	Dissociating group
$H_4L \leftrightarrow H_3L^- + H^+$	8,17 ± 0,15	7-OH
$H_3L^- \leftrightarrow H_2L^{2-} + H^+$	9,63 ± 0,16	3'-OH
$H_2L^{2-} \leftrightarrow HL^{3-} + H^+$	10,76 ± 0,14	5-OH
$HL^{3-} \leftrightarrow L^{4-} + H^+$	11,85 ± 0,26	4'-OH

It should be noted that the calculated dissociation constants of the OH groups of rutin differ slightly from the pK values given in [36,37] due to the use of different solvents (methanol or water)

Thus, the analysis of electronic absorption spectra shows that the dissociation of the hydroxyl groups of rutin in aqueous-ethanolic solutions takes place in the order: 7-OH, 3′-OH, 5-OH, 4′-OH.

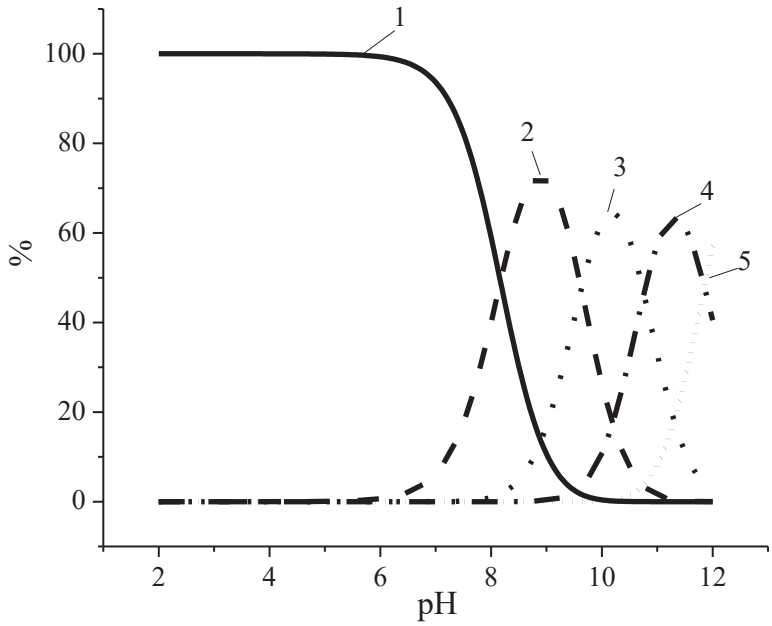

Fig.3 Dissociation diagram of rutin: H_4L undissociated form of rutin (1); H_3L^- (2); H_2L^{2-} (3); HL^{3-} (4), L^{4-} (5).

The study of complex formation processes of rutin with Co (II) and Cu (II) ions was performed by pH-potentiometric titration. Figure 4 shows titration curves of the Co(II):Rut (a) and Cu(II):Rut (b) systems, which are in a more acidic pH range relative to the critical titration of rutin, which is associated with the formation of metal complexes with functional groups Rut (carbonyl –CO= or –OH). The titration curves of cobalt and copper systems at M: Rut = 1: 1 (Fig. 4, curves 2) have almost the same appearance: two poorly defined buffer regions (pH ~ 6-8 and 8-10) and a blurred jump at pH ~ 10. It is likely that tapered complexes are formed in a more acidic medium in which the metals are bonded to the 5-hydroxyl and 4-carbonyl groups of rings A and C. In an alkaline medium, the metals are bonded to the deprotonated hydroxyls of the catechol moiety. The titration curve of the system

Cu(II):Rut = 2:1 (Fig. 4, curve 3) has two distinct jumps (pH 5.5 and 9), shifted to a more acidic pH region compared to the equimolar system. Under these conditions, the interaction of a copper ion with the 3′-4′-hydroxyl groups of the ring B of two rutin molecules is possible similar to the interaction of Cu (II) with quercetin [38].

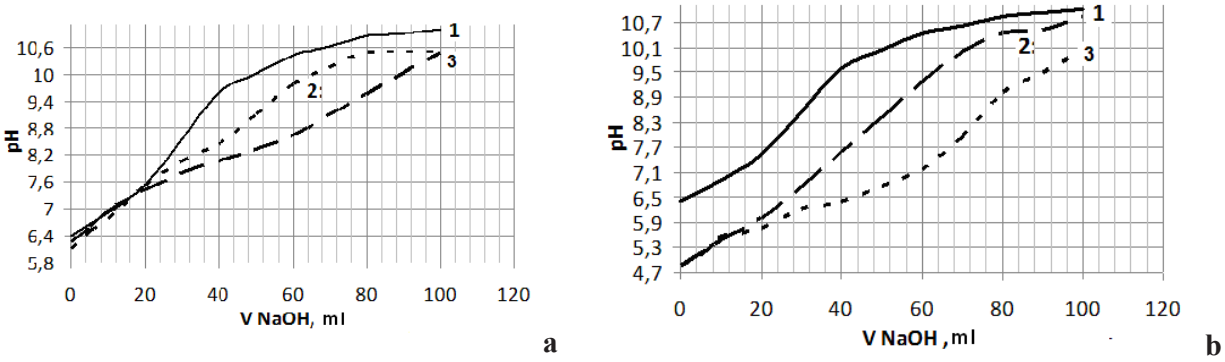

Fig. 4. Curves of pH-metric titration of the systems Co(II):Rut (a) and Cu (II):Rut (b): 1. – Rut; 2. – M:Rut = 1:1; 3. – M:Rut = 2: 1.

Based on the obtained titration curves, the concentration of the free ligand [L^-] and the formation function were calculated using the formulas:

$$-\lg[L^-] = pk_a - pa_{H+} - \lg(C_L - C_T - a_{H+}), \quad (1)$$

$$\tilde{n} = (C_T + a_{H+} - [L^-]) / C_M, \quad (2)$$

where C_L – the total ligand concentration, C_M – the total metal concentration, C_T – the concentration of added titrant, a_{H+} – the activity of hydrogen ions, k_a – the acid dissociation constant of rutin.

Based on the values of ñ according to the Bjerrum method [39] stepwise stability constants of complexes of cobalt and copper with rutin are calculated (Table 2).

The stability of Co(II) complexes is several orders of magnitude lower than the stability of copper complexes, which is obviously due to the high affinity of Cu^{2+} for rutin donor oxygen atoms, and especially for the ortho-dihydroxyl group [34].

Table 2

The calculated values of the stability constants of complexes of Co (II) and Cu (II) with rutin*.

Metals	M: Rut	lgβ
Co^{2+}	1:1	8,85±0,05
	2:1	8,16±0,07
Cu^{2+}	1:1	18,51±0,08
	2: 1	11,76±0,05

**lgβ is given for the form of complexes [ML] and [M_2L]*

The complexation of rutin with Co(II) and Cu(II) ions was analyzed using electronic absorption spectra in the ultraviolet and visible regions depending on pH (fig. 5, a, b)

In the spectra of all studied systems with a change in pH and the ratio of components, there are a change in the optical density of solutions and a bathochromic shift of the absorption maxima of bands I and II in complexes relative to their position in the spectra of

pure rutin. This indicates complexation in M: Rut systems. It should be noted that in acidic media (pH <4) rutin is in the protonated form H_4L, the participation of which in complexation is not possible. At pH≥6, rutin turns into an electron-donating form, which further dissociates with the formation of a flavonolate ion and can interact with the metal-complexing agent. The largest bathochromic shift λmax for all studied systems occurs at pH≥5.5 due to the involvement in chelation of different binding sites.

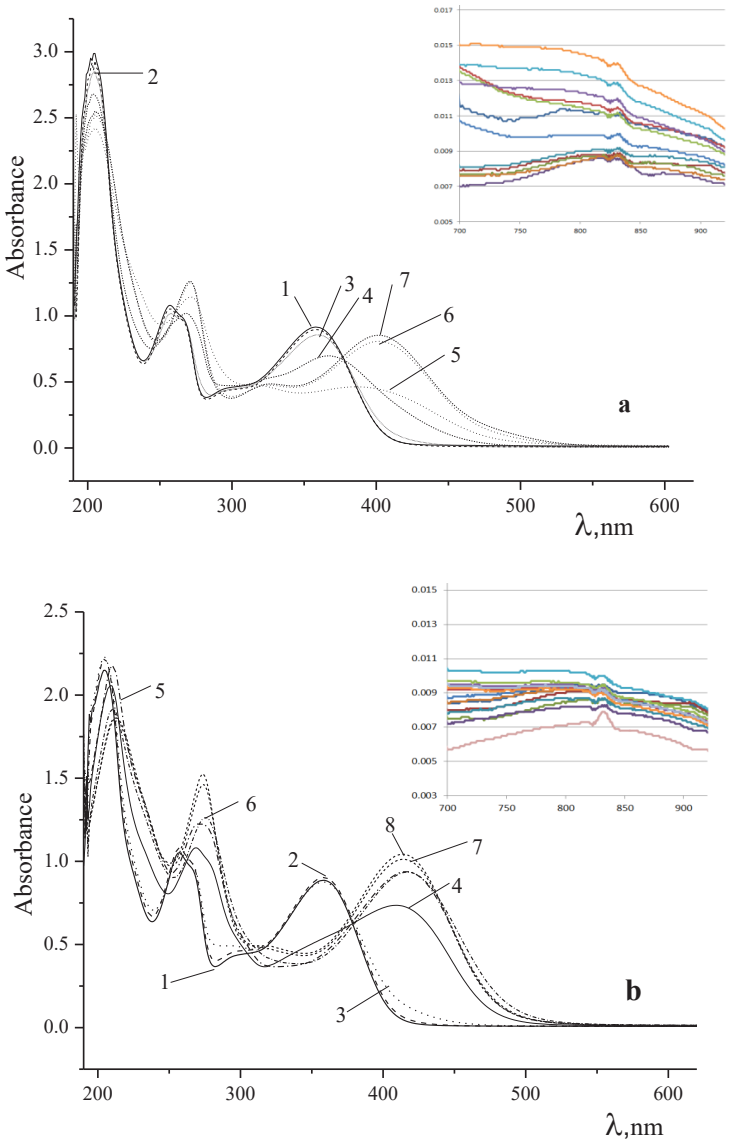

Fig. 5 UV spectra of systems as a function of pH: a – Co: Rut=1:1 (2.56 (1); 4.16 (2); 6.5 (3); 7.52 (4); 8.44 (5); 9.79 (6); 10.48 (7)); b – Cu:Rut=2:1 (2.6 (1); 3.67 (2); 4.62 (3); 5.55 (4); 6.38 (5); 7.95 (6); 9.47 (7); 10.0 (8)). Insertion: UV spectra of systems in the range of 700–900 nm.

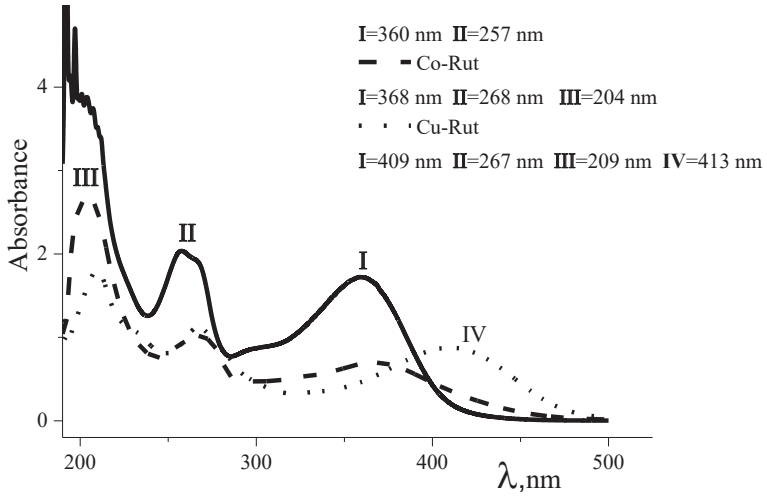

Fig.6 UV spectra of rutin and complexes CoRut, CuRut.

Regardless of the metal, for all systems, the maximum of band I shifts toward long wavelengths compared to the solution of pure rutin (Fig. 6).

For a Cu-containing system, band I is strongly shifted to the visible region by 53 nm ($\lambda_{max.}$ = 413 nm, band IV). Under similar conditions, band II of rutin in the presence of metal ions has a bathochromic shift of ~ 10 nm, but in the spectra of metal complexes appears band III at 204 (209) nm, which may be due to different modes of coordination of cations to the functional groups of rutin.

Figure 7 shows a comparison of electronic absorption spectra for systems with different M: Rut ratios.

In the UV spectra of copper complexes with the Cu:L=2:1 ratio for bands II and I, a hypsochromic shift relative to equimolar metal complex (λ_I 277 → 267 nm; λ_{II} 420 → 409 nm) is observed, which can be explained by the different structure of metal complex and an increase in conjugation in the heterocyclic ring. Probably, at the ratio Cu:L=1:1, chelation occurs at the 5-OH hydroxyl group and the oxygen atom of the carbonyl group (4-C=O) of the C-ring of rutin. The maximum absorption responsible for the absorption of the A-ring of rutin (7-OH) for both systems does not actually change (210 nm), which indicates that the 7-OH group does not participate in complexation due to its lower protic acidity. The formation of copper complexes with a ratio of 2:1 occurs both due to 5-OH and 4C=O and due to two hydroxo groups of the catechol fragment. The different structures of the complexes are confirmed by the change in the values of optical density as a function of the pH of solutions (fig. 7a, inset). The catechol group is the most likely metal binding site, especially in alkaline media (pH ≥9) due to the deprotonation of hydroxyls. At the ratio Cu: Rut = 2: 1, the copper ion can bind to the hydroxyls of the catechol groups from two rutin molecules, which are located in orthogonal planes. The different mode of coordination of Cu(II) is also evidenced by the position of the bands of the d – d transition $B_{1g} \rightarrow A_{1g}$, corresponding to planar-square complexes: 644 nm (2:1) and 634 nm (1:1).

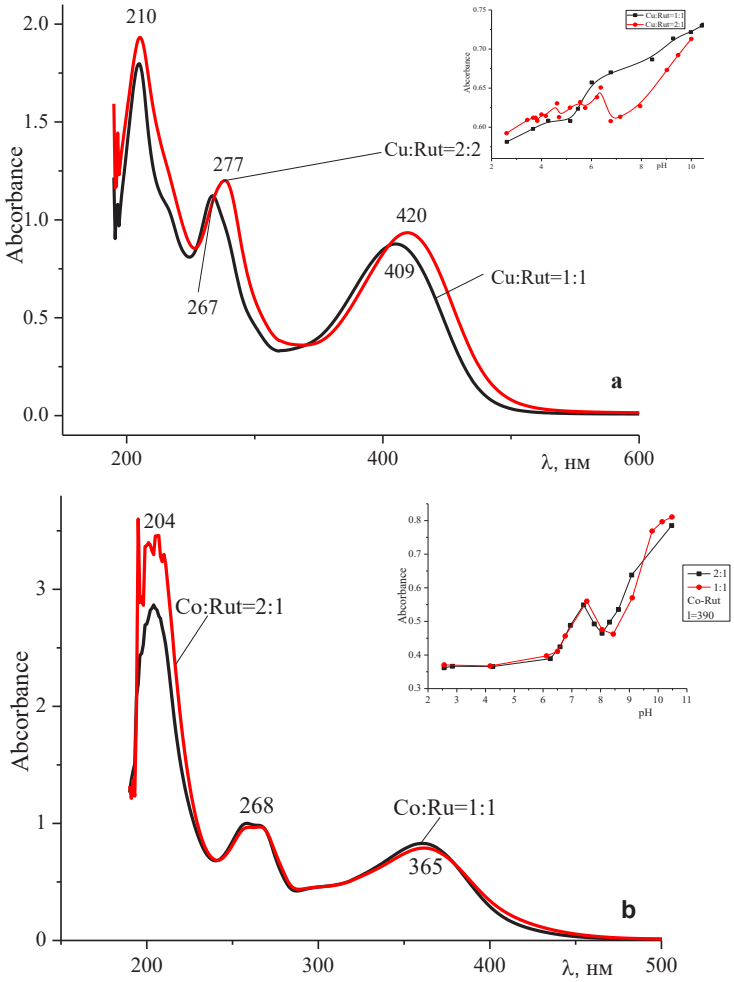

Fig. 7 Comparison of UV spectra for systems with different Cu:Rut (a), Co:Rut (b) rations (pH=6).

Insert: dependence of optical density on pH at ratios M:Rut = 1:1; 2:1 In the electronic absorption spectra of Co(II) complexes, regardless of the Co: Rut ratio, the maxima of the absorption bands are at the same wavelength, and the course of the A → pH curves is the same (fig. 7, b). This indicates the formation of complexes of the same composition in both systems. However, at a ratio of 2:1, the spectral bands are split into 3 components, which may be associated with the formation of biligand complexes in which the Co^{2+} ion is coordinated through the catechol fragment B of the ring of each rutin molecule. In this case, the cobalt ion is in a distorted octahedral environment, as evidenced by the maxima of the d-d transitions in the electronic absorption spectra corresponding to the $^4T_{1g}(F) \rightarrow {}^4T_{1g}(P)$ transition in high-spin six-coordinate complexes of cobalt(II) (λ_{max}=508 (1:1) and 512 (2:1) nm). The bathochromic shift λ_{max} in the 2:1 system is due to the formation of a tetragonally deformed octahedron of D_{4h} symmetry due to a significant spin-orbit interaction in the excited state $^4T_{1g}(P)$.

According to the results of electrospray mass spectrometry, the composition of the products formed in the studied systems was determined (tabl. 3).

Table 3

The mass-to-charge ratio of fragments and their interpretation in the ESI mass spectrum of the Co (II) and Cu (II) complexes with Rut.

m/z				Interpretation
Co(II):Rut		Cu (II):Rut		
1:1	2:1	1:1	2:1	
611	611	611	611	$(L+H)^+$
	633	-	636	$[Na^I(L)]^+$
668	668	672	672	$[M^{II}(L-H)]^+$
726	725	-	738	$[M_2^{II}(L-H_{5,3',4'})]^+$
	1278		1282	$[M^{II}(L-H_{3',4'})L]^+$

The peak of protonated flavonoid (m/z= 611) is observed in all spectra. In the mass spectra of the M:Rut = 2:1 systems, quite intense peaks with m/z=633 and 636 appear, which correspond to the salts of rutin with Na. In addition, the ESI MS identified key characteristic fragments with m/z=668 (for Co) and 672 (for Cu), which correspond to species $[M^{II}(L - H)]^+$, which clearly indicates the formation of metal complexes with monodeprotonated rutine molecules. In this case, the peak of the $[M^{II}(L - H)]^+$ ion is the main one in the studied mass spectra. Also in the mass spectra there is a weakly intense peak with m/z = 726 (738), which corresponds to the formation of dimeric cations $[M_2^{II}(L\text{-}H_{5,3',4'})]^+$, in which 3-d metals are coordinated by deprotonated catecholic hydroxo-groups of the ligand. In ESI MS, peaks of biligand complexes $[M^{II}(L\text{-}H_{3',4'})L]^+$ with the inclusion of one neutral rutin molecule are recorded. Moreover, the intensity of these peaks is quite small.

CONCLUSIONS. Complex formation has been studied in the systems M (II) - Rut (M (II) = Co (II), Cu (II)) in aqueous alcohol solutions depending on pH and the ratio metal: ligand = 1 :1; 2: 1. It was shown that the structure and stoichiometric composition of the complexation reaction products are influenced by such basic parameters as L:M and the pH value of the medium. Depending on the pH value, chelation involves certain binding sites, which primarily is associated with the redistribution of the electron density in the flavonoid molecule.

In a weakly acidic or neutral medium, regardless of the M(II): Rut ratio, the formation of monoligand complexes of rutin with 3-d metals occurs with the participation of 5-OH and 4-C=O fragments of the A and C rings, and in an alkaline medium, chelation proceeds on the catecholic fragment of ring B rutin. Biligand complexes are formed with the participation of the gydroxo groups of the catechol fragment of each rutin molecule, and the formation of compounds with a ratio of 2:1 occurs both due to 5-OH and 4C=O and due to 3 ', 4'-OH groups. The calculated values of the stability constants of the complexes showed that the stability of the Co (II) complexes is several orders of magnitude lower than the stability of the corresponding Cu (II) complexes.

ACKNOWLEDGEMENTS

This work was supported by funding from the National Academy of Sciences of Ukraine (318 E – program), «Creation of new multifunctional nanomaterials based on coordination compounds of 3d-metals and lanthanides with O, N-donor ligands».

СПЕКТРОСКОПІЧНІ ДОСЛІДЖЕННЯ КОМПЛЕКСІВ Cu(II) ТА Co(II) З РУТИНОМ У РОЗЧИНІ

О. К. Трунова*, М. С. Артамонов, Т. О. Макотрик

Інститут загальної та неорганічної хімії ім. В. І. Вернадського НАН України, просп. Академіка Палладіна, 32/34, Київ 03142, Україна
** e-mail: trelkon@gmail.com.*

Методами електронної спектроскопії поглинання та pH-метричного титрування вивчено комплексоутворення в системах M(II) – рутин (Rut) (M(II) = Co, Cu) у водно-етанольних розчинах залежно від співвідношення метал:ліганд (1:1; 2: 1) і pH середовища. Показано, що на структуру та стехіометричний склад продуктів реакції комплексоутворення впливають такі основні параметри, як L:M та значення pH середовища. Залежно від значення pH, в хелатуванні беруть участь певні сайти зв'язування, що, перш за все, пов'язано із перерозподілом електронної густини в молекулі флавоноїду. У слабокислому або нейтральному середовищі, незалежно від співвідношення M(II):Rut, утворення монолігандних комплексів рутину з 3-d-металами відбувається за участю 5-OH і 4-C=O фрагментів A і C кільця, а в лужному середовищі хелатування відбувається на катехольному фрагменті кільця B рутину. Білігандні комплекси утворюються за участю гідроксогруп катехольного фрагменту кожної молекули рутину, а утворення сполук у співвідношенні 2:1 відбувається як за рахунок 5-OH і 4C=O, так і за рахунок 3', 4'-OH груп. Розраховані значення констант стійкості комплексів показали, що стійкість комплексів Co(II) на кілька порядків нижча за стійкість відповідних комплексів Cu(II).

Ключові слова: комплекс, мідь, кобальт, рутин, флавоноїди, електронна спектроскопія.

REFERENCES

1. Chebil L., Humeau C., Anthoni J., Dehez F., Engasser J.-M., Ghoul M. Solubility of Flavonoids in Organic Solvents. *J. Chem. Eng.* 2007. **52**: 1552.
2. Tarakhovsky Yu.S., Kim Yu.A., Abdrasilov B.S., Muzafarov E.N. *Flavonoids: biochemistry, biophysics, medicine* (Pushchino: Synchrobook, 2013) [in Russian].
3. Malesev D., Kuntic V. Investigation of metal-flavonoid chelates and the determination of flavonoids via metal-flavonoid complexing reactions. *J. Serb. Chem. Soc.* 2007, **72**: 921.
4. Oyvind M., Kenneth R. Markham Andersen *Flavonoids: Chemistry, Biochemistry and Applications*.(CRC Press Taylor & Francis Group, 2006).
5. Heim K.E., Tagliaferro A.R., Bobilya D. J. Flavonoid antioxidants: chemistry, metabolism and structure-activity relationships. *J. Nutrit. Biochem*. 2002.**13**: 572.
6. Cushnie T.P., Lamb A.J. Antimicrobial activity of flavonoids. *J Antimicrob Agents*. 2005. **26** (5): 343.
7. Yang J., Guo J., Yuan J. In vitro antioxidant properties of rutin. *Food Science and Technology.* 2008. **41** (6): 1060.
8. Crozier A., Jaganath I.B., Clifford M.N. Dietary phenolics: chemistry, bioavailability and effects on health. *Nat Prod Rep.* 2009. **26**: 1001.
9. Marzena Symonowicz, Mateusz Kolanek. Flavonoids and their properties to form chelate Complexes. *Biotechnol Food Sci*. 2012. **76** (1): 35–41.

10. Al-Dhabi, N. A., Arasu, M. V., Park, C. H., & Park, S. U. An up-to-date review of rutin and its biological and pharmacological activities. *EXCLI journal*. 2015. **14**: 59.
11. Ganeshpurkar A., Saluja A.K. The pharmacological potential of rutin. *Saudi pharmaceutical J.* 2017 **25** (2): 149.
12. Kuzniak A., Pusz J., Maciolek U. Potentiometric study of Pd (II) complexes of some flavonoids in water-methanol-1, 4-dioxane-acetonitrile (MDM) mixture. *Acta poloniae pharmaceutica.* 2017. **74** (2): 369.
13. Erkoc S., Erkoc F., Keskin N. Theoretical investigation of quercetin and its radical isomers. J. *Mol. Struct. Theochem*. 2003. **631**: 141.
14. Satterfield M. Brodbelt J.S. Enhanced Detection of Flavonoids by Metal Complexation and Electrospray Ionization Mass Spectrometry. *Anal. Chem.* 2000. – P. 5898–5906.
15. Kasprzak M. M., Erxleben A., Ochocki J. Properties and applications of flavonoid metal complexes. *RSC Advances*. 2015 **5**(57): 45853.
16. Hu Y.J., Yue H.L., Li X.L., Zhang S.S., Tang E., Zhang L.P. () Molecular spectroscopic studies on the interaction of morin with bovine serum albumin. *J.Photochem.Photobiol.B*. 2012. **112**: 16.
17. Grazul M., Budzisz E. Biological activity of metal ions complexes of chromones, coumarins and flavones. *Coordin.Chem*. 2009. **83**: 363.
18. Ravishankar D., Rajora A.K., Greco F., Osborn H.M. (). Flavonoids as prospective compounds for anti-cancer therapy. *The international journal of bioch. & cell biology.* 2013. **45** (12): 2821.
19. Selvaraj S., Krishnaswamy S., Devashya V., Sethuraman S., Krishnan U.M. Flavonoid–metal ion complexes: a novel class of therapeutic agents. *Medicinal Research Reviews*, 2014. **34**(4): 677.
20. Kostyuk V.A., Potapovich A.I., Vladykovskaya E.N., Korkina L.G., Afanas'ev I.B. Influence of metal ions on flavonoid protection against asbestos-induced cell injury. *Arch Biochem Biophy*. 2001. (385): 129.
21. De Souza R.F., Sussuchi E.M., De GiovaniW.F. (). Synthesis, electrochemical, spectral, and antioxidant properties of complexes of flavonoids with metal ions. *Synthesis and reactivity in inorganic and metal-organic chemistry*. 2003. **33** (7): 1125.
22. Bratu M.M., Birghila S.E.M.A.G.H.I U.L., Miresan H., Negreanu-Pirjol T., Prajitura C., Calinescu M. Biological activities of Zn (II) and Cu (II) complexes with quercetin and rutin: Antioxidant properties and UV-protection capacity. *Rev. Chim.(Bucharest).* 2014. **65**: 544.
22. Khater M., Ravishankar D., Greco F., Osborn H. Metal complexes of flavonoids: their synthesis, characterization, and enhanced anti-oxidant and anti-cancer activities. *Future Medicinal Chemistry* 2019. **11** (21): 2845.
23. Brown J.E., Khodor H, Hider R.C., Rice-Evans C.A. Structural dependence of flavonoid interactions with Cu^{2+} ions: implications for their antioxidant properties. *Biochemical Journal.* 1998. **330** (3): 1173.
24. Anafas'ev I.B., Ostrakhovitch E.A., Mikhal V., Ibragimova L., Korkina G.A. Enhancement of antioxidant and anti-inflammatory activities of bioflavonoid rutin by complexation with transition metals. *Biochem Pharmacol.* 2001. **61**: 677.
25. Takamura K., Sakamoto M. Spectrophotometric Studies on flavonoid-Copper(II) Complexes in Methanol Solution. *Chem. Pharm. Bull.* 1978. **26** (8): 2291.
26. Malešev D., Radović Z., Jelikić-Stankov M., Bogavac M. Investigation of Molybdate(II)-Rutin Complex and the Determination of theDissociation Constant of Rutin in Water-Ethanol Mixture. *Analytical Letters*. 1991. **24** (7): 1159.
27. Kuzniak A., Pusz J., Maciolek U. (). Potentiometric study of Pd (II) complexes of some flavonoids in water-methanol-1, 4-dioxane-acetonitrile (MDM) mixture. *Acta poloniae pharmaceutica.* 2017. **74**(2): 369.
28. Zhang L., Liu Y., Wang Y., Xu M., Hu X. UV–Vis spectroscopy combined with chemometric

study on the interactions of three dietary flavonoids with copper ions. *Food chemistry*. 2018. **263**: 208.
29. Peng B., Li R., Yan W. Solubility of rutin in ethanol+ water at (273.15 to 323.15) K. *Journal of Chemical & Engineering Data*. 2009. **54**(4): 1378.
30. Zi J., Peng B., Yan W. Solubilities of rutin in eight solvents at T=283.15, 298.15, 313.15, 323.15, and 333.15 K. *Fluid Phase Equilibria.* 2007. **261**(1–2): 111.
31. Williams D., *Metals of Life* . (M.: Mir, 1975) [in Russian].
32. Pribil R., *Komplexone in der chemischen Analyse* (VEB Deutscher Verlag der Wissenschaften, Berlin, 1961).
33. Saprykova Z.A. Boos G.A., Zakharov A.V. Physicochemical methods for the study of coordination compounds in solutions (Kazan: Publishing House. Kazan University, 1988) [in Russian].
34. Bukhari S.B., Memon S., Mahroof Tahir M., Bhanger M.I. () Synthesis, characterization and antioxidant activity copper-quercetin complex. *Spectrochim. Acta Part A: Molecular and Biomolecular Spectroscopy*. 2009. **71**(5): 1901.
35. Kholin Yu.V. *Quantitative physicochemical analysis of complexation in solutions and on the surface of chemically modified silicas: meaningful models, mathematical methods and their applications.* – (Kharkiv: Folio, 2000) [in Russian].
36. Graciela M. Escandar, Luis F. Sala Complexing behavior of rutin and quercetin. *Can. J. Chem.* 1991. **69** (12): 1994.
37. Lipkovska N.A., Barvinchenko V.N., Fedyanina T.V., Rugal A.A. Physicochemical Properties of Quercetin and Rutin in Aqueous Solutions of Decamethoxin Antiseptic Drug. *Russian Journal of Applied Chemistry*. 2014. **87** (1): 36.
38. Torreggani A., Tamba M., Trinchero A., Bonora S. Copper (II)-Quercetin complexes in aqueous solutions: spectroscopic and kinetic properties. *J. Molec. Struct.* 2005. **744**: 759.
39. Bjerrum Ya. *Formation of metal amines in an aqueous solution (Theory of reversible step reactions)*. (M.: IL, 1961) [in Russian].

Стаття надійшла 16.11.2021.

УДК: 546.650:547.639.5:535.37 doi: 10.33609/2708-129X.87.10.2021.103-115

STRUCTURE AND SPECTRAL-LUMUINESCENT PROPERTIES OF LANTHANIDE-CONTAINING COMPLEXES WITH AZACROWN CALIXARENES

Smola S.S.[1], Rusakova N.V.[1], Alekseeva O.A.[1], Basok S.S.[1], Kirichenko T.I.[1], Korovin O.Yu.[1], Malinka O.V.[2], Semenyshyn N.N.[1]

[1]A.V. Bogatsky Physico-chemical Institute, National Academy of Sciences of Ukraine, 86, Lustdorfskaya doroga, 65080 Odessa, Ukraine
[2]Odessa National Academy of Food Technology, 112, Kanatna Street, 65039 Odessa, Ukraine
email: sssmola@gmail.com

Lanthanide complexes with calix[4]arenes lower rim substituted with two azacrown ether fragments are reported. The size of the substituent cavity varied from 4 to 6 heteroatoms. The complexes were analyzed by means of IR, NMR, ESI mass spectroscopy. It is assumed that the coordination of Ln(III) ions occurs through the donor atoms of the lower rim; the counter anion and solvent molecule are also coordinated. Lanthanide-centered characteristic luminescence was observed in Eu(III), Tb(III) and Yb(III) complexes. The most efficient *4f*-luminescence is observed for terbium-containing complexes with benzo-crown-derived ligands. The pathways of the sensitization of 4f-luminescence are discussed.

Keywords: lanthanide complexes, calix[4]arenes, azacrown ethers, luminescence.

INTRODUCTION. Calix[4]arenes can be considered as universal building blocks, as their molecules have a characteristic feature – the presence of two «rims», which can be modified by functional groups of different nature, and a hydrophobic cavity as an additional binding site. The functionalization of the calix[4]arene macrocycle with polydentate substituents purposefully influences the complexing properties, including the possibilities of the preparation of mono- or heteronuclear complexes of various compositions. Particular interest is shown in the design of calix[4] arenes lower rim substituted with crown ether fragments. Such combination increases the coordination ability of calixarenes, reduces their conformational mobility and can be used for ion and molecular recognition [1–3].

As a rule, lanthanide-calix[4]arene complexes are formed through coordinating groups at the lower rim which is easily achieved by the functionalization of phenolic OH groups. The first structures of mono- and binuclear europium-containing compounds with *p-tert*-butyl-calix[4]arene and its derivatives both in solid state and in solutions were reported by J.M. Harrowfield and coworkers in the 1985–1990s [4–6]. In subsequent works, with the

development of synthetic procedures, both the range of functionalized ligands and the number of lanthanide ions were increased. The general method of synthesis consists in the interaction of lanthanide salts (most often chlorides, nitrates, or picrates) and calix[4]arenes in an anhydrous solvent or in a mixture of solvents in the presence of triethylamine. The latter, as in the case of other metals, promotes the dissociation of phenolic groups, thereby facilitating the formation of complexes.

4f-Luminescence in lanthanide complexes with a number of calix[4]arenes is caused by intramolecular energy transfer from the organic part of the molecule to the metal ion. It can be assumed that it manifests itself in such compounds as crown-calix[4]arenes, while the lanthanide ion can be coordinated by both calix[4]arene and crown ether fragments. The number of studies on the spectral luminescent properties of complexes of such compounds with lanthanide ions is rather low. In the present work, we report our study of the spectral luminescent properties of lanthanide complexes with calix[4]arene derivatives substituted with two azacrown ether fragments. The size of the substituent cavity varied from 4 to 6 heteroatoms.

EXPERIMENT AND DISCUSSION OF THE RESULTS. Calix[4]arenes L^1H_2 – L^7H_2 [7, 8] (Table 1) and the corresponding lanthanide-containing complexes were synthesized according to the methods described in [9, 10] in the presence of equimolar quantities of triethylamine. Complexes were isolated in solid state and identified by means of elemental analysis, mass spectrometry, IR, ^{1}H NMR spectroscopy. The geometry optimization of the structures of complexes was performed by the methods of molecular mechanics (HyperChem, MM+).

The absorption spectra in the UV and visible regions were recorded on a spectrophotometer Ulab S261UV in 10 mm quartz cuvettes, and in the IR region (4000–400 cm^{-1}) on a Shimadzu FT-IR8400S spectrophotometer (in KBr pellets).

Fluorescence excitation and emission spectra, as well as phosphorescence and 4f-luminescence were recorded on a Fluorolog FL 3-22 spectrofluorimeter (Horiba Jobin Yvon, Xe-450 W ozone-free lamp) equipped with a photomultiplier R928P (Hamamatsu, Japan) for the visible spectral region and a liquid nitrogen cooled InGaAs detector (DSS-IGA020L, Electro-Optical Systems, Inc.) for the NIR.

The values of the singlet (E_S) and triplet levels (E_T) of the derivatives of calix[4]arenes and lutetium-containing complexes were determined by a known procedure [11] at 77K using phosphorescence spectra obtained with different time delays after the excitation pulse ceased. The values of the relative quantum yield of 4f-luminescence (φ) of lanthanide ions (measurement error ± 20%) in complexes were calculated as in [11, 12]. The number of coordinated solvent molecules in complexes was estimated using the Horrocks and Sudnick method [13, 14].

The studied compounds can be divided into two groups. The first consists of calix[4]arene macrocycles linked to azacrown ether by an amide bond (L^1H_2 - L^4H_2) and the second consists of their reduced analogs (L^5H_2 - L^7H_2). The complexes with the ratio Ln:L^nH_2 = 1:1, in which f-cations are coordinated by the donor OH-groups of calix[4]arene, were obtained by the equimolar interaction of the starting materials. Excess of lanthanide salt provides sandwich structures with the 2:1 ratio.

Table 1

Calix[4]arenes modified with azacrown ethers, used in this work.

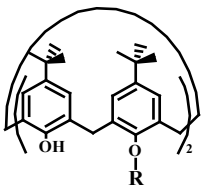

Ligand	Nomenclature name	R
L^1H_2	5,11,17,23-tetra-*tert*-butyl-25,27-bis[(1,4,7-trioxa-10-azacyclododec-10-yl)carbonylmethoxy]-26,28-dihydroxycalix[4]arene	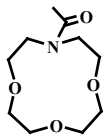
L^2H_2	5,11,17,23-tetra-*tert*-butyl-25,27-bis[(1,4,7,10-tetraoxa-13-azacyclopentadec-13-yl)carbonylmethoxy]-26,28-dihydroxycalix[4]arene	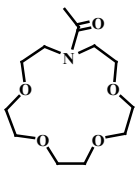
L^3H_2	5,11,17,23-tetra-*tert*-butyl-25,27-bis[(6,7,9,10,12,13,15,16-octahydro-5,8,14,17-tetraoxa-11-azabenzocyclopentadecen-11-yl) carbonylmethoxy]-26,28-dihydroxycalix[4]arene	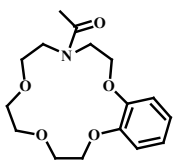
L^4H_2	5,11,17,23-tetra-*tert*-butyl-25,27-bis[(1,4,7,10,13-pentaoxa-16-azacyclooctadec-16-yl)carbonylmethoxy]-26,28-dihydroxycalix[4]arene	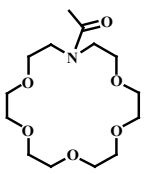
L^5H_2	5,11,17,23-tetra-*tert*-butyl-25,27-bis[(1,4,7-trioxa-10-azacyclododec-10-yl)ethoxy]-26,28-dihydroxycalix[4]arene	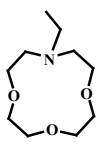
L^6H_2	5,11,17,23-tetra-*tert*-butyl-25,27-bis[(1,4,7,10-tetraoxa-13-azacyclopentadec-13-yl)ethoxy]-26,28-dihydroxycalix[4]arene	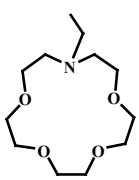
L^7H_2	5,11,17,23-tetra-*tert*-butyl-25,27-bis[(1,4,7,10,13-pentaoxa-16-azacyclooctadec-16-yl)ethoxy]-26,28-dihydroxycalix[4]arene	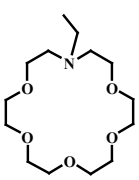

The obtained compounds were analyzed by physico-chemical methods. The ESI mass spectra of all complexes contain peaks of molecular ions corresponding to mononuclear blocks. As an example, Fig. 1 shows a mass spectrum of a lutetium-containing complex with L^2H_2, which contains the peak of a molecular ion (m/z = 1414), which indicates the presence of a chloride anion and one solvent molecule in the complex. The peaks with a lower m/z value correspond to fragments without acetonitrile molecule, chlorine atom, and one or two azacrown ether fragments (peaks with m / z = 1375, 1340, 1123, and 906, respectively).

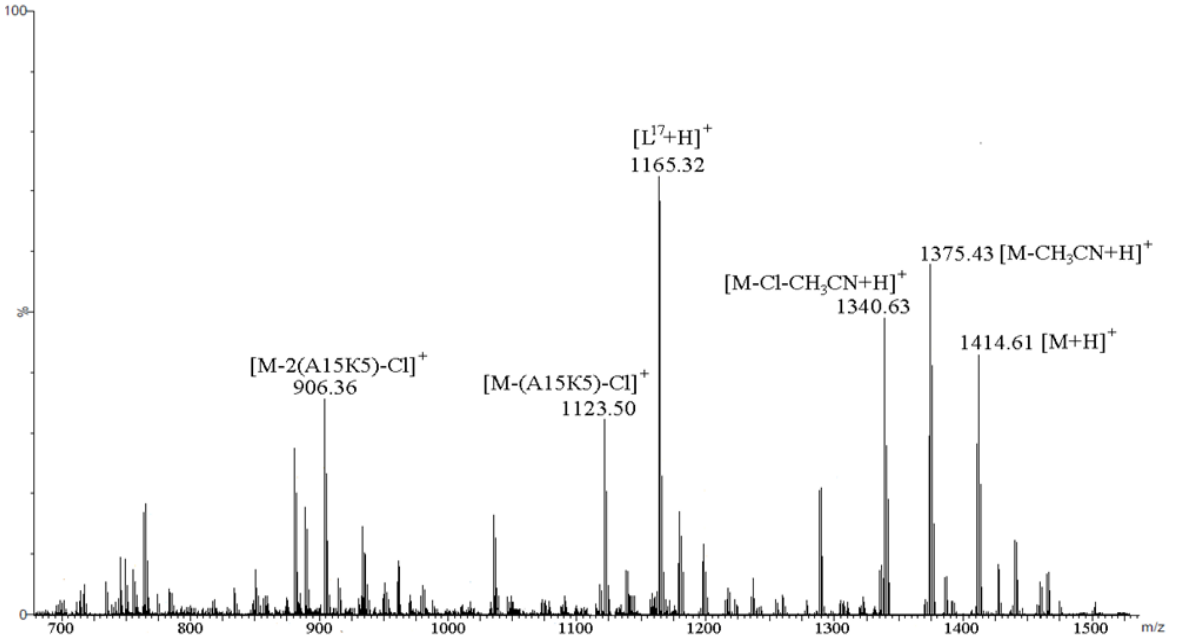

Fig. 1. ESI-mass spectrum of $[LuL^2Cl(CH_3CN)]$.

The coordination of lanthanide ions by the donor groups of calix[4]arene is confirmed by IR spectroscopy data. The vibration band of the OH groups of the starting calix[4]arenes (ν(O-H) = 3150–3250 cm^{-1}) is absent in the spectra of all complexes. In the spectra of complexes with $L^{1\text{-}4}H_2$, the vibration bands of carbonyl groups with maxima in the range of 1640–1690 cm^{-1} undergo a low-frequency shift of 20–30 cm^{-1}, which indicates their participation in the coordination of the metal ion. The vibration band of the ether bonds of the lower rim of calix[4]arene (ν(C-O) = 1030–1040 cm^{-1}) is shifted to the low-frequency region by 50–60 cm^{-1} in comparison with the spectra of the initial compounds. At the same time, the vibration bands of the ether groups of azacrown substituents ($\nu(C_{crown}\text{-}O)$ = 1125–1135 cm^{-1}) do not change. The formation of complexes is also evidenced by the appearance of a low-frequency band at 450–460 cm^{-1}, which refers to the vibrations of lanthanide-oxygen bonds. The position and intensity of the remaining bands in the spectra of complexes do not undergo significant changes in comparison with the spectra of the starting compounds.

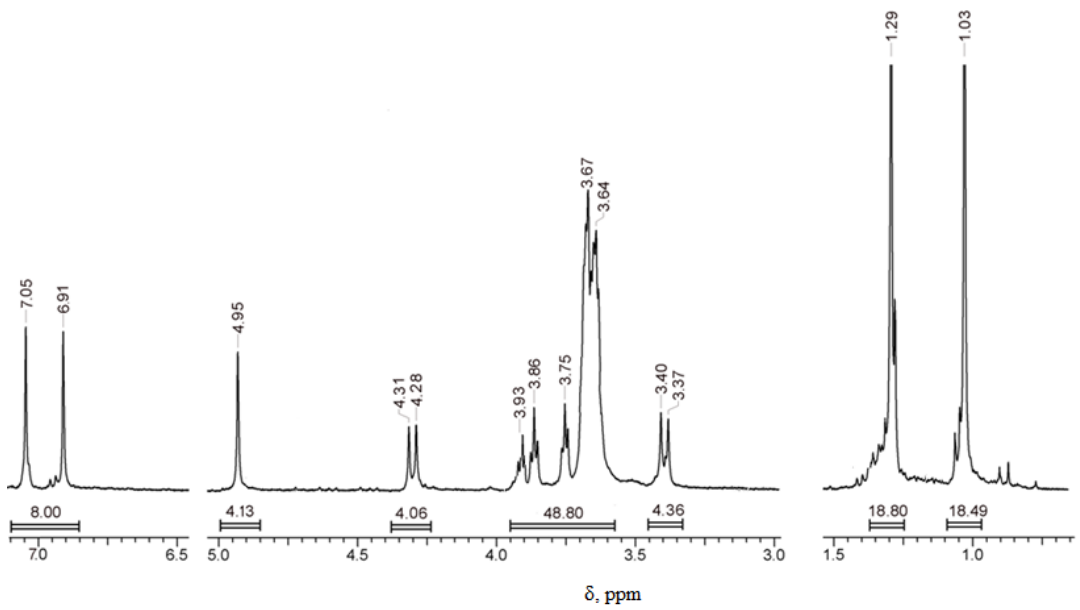

Fig. 2. ^{1}H NMR spectrum [LuL^{3}Cl(CH$_3$CN)] (CDCl$_3$, 25 °C).

A ^{1}H NMR spectrum of the [LuL^{4}Cl(CH$_3$CN)] complex as an example is shown in Fig. 2. The signals of the protons of phenyl hydroxo groups, which are at 7.50–7.70 ppm in the spectra of free ligands, disappear upon complexation, which indicates their substitution.

All signals corresponding to the calix[4] arene macrocycle are shifted: the signals of aryl protons and the protons of *tert*-butyl groups are shifted downfield by 0.09–0.11 and 0.05–0.08 ppm, respectively, and the doublets from methylene bridges, which are in the spectra of calixarenes at 3.28 and 4.44 ppm, shift towards each other by 0.09–0.15 ppm, which indicates a smaller flattening of the calix[4]arene conformation in the complex. The participation of the carbonyl oxygen atoms of the amide group in coordination is confirmed by the shift of the δ(OCH$_2$CO) signals of 0.08–0.13 ppm, as well as the appearance of a triplet of N-CH$_2$ groups at 3.87–3.95 ppm. The position of the signals of the remaining protons of the azacrown ether substituent in the range 3.60–3.70 ppm does not change. As for amine derivatives (complexes with L^{5}H$_2$ – L^{7}H$_2$), small changes in the intensity of the main signals of the methylene groups of azacrown ethers in the region of 3.55–4.10 ppm probably indicate the formation of a system of intra- and intermolecular hydrogen bonds.

The data obtained and the MM$^+$ calculations (Fig. 3) allowed us to conclude that in the complexes with L^{1}H$_2$ – L^{4}H$_2$ compounds, the coordination polyhedron of lanthanide is formed by four oxygen atoms of the lower rim and carbonyl groups. Considering the coordination of the counterion of lanthanide salt and one solvent molecule (acetonitrile), the coordination number of lanthanide ion in complexes is 8. As for the complexes with calix[4] arenes L^{5}H$_2$ – L^{7}H$_2$, the coordination site of the lanthanide ion consists of four oxygen atoms of the lower rim of calix[4]arene, the chloride anion, and the solvent molecule, the coordination number of Ln(III) is 6.

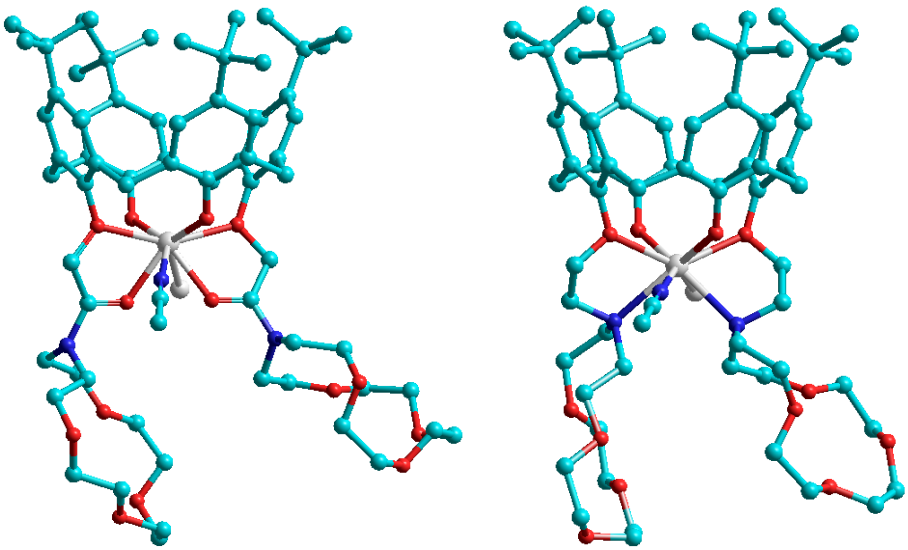

Fig. 3. Calculated spatial models of Ln(III) complexes with L^2H_2 (left) and L^6H_2 (right) (hydrogen atoms are omitted).

The absorption spectra of lanthanide complexes with azacrown ether-functionalized calix[4]arenes are characterized by three bands. The introduction of substituents leads to the appearance of an additional band in the region λ_{max} = 270–275 nm (37040–36360 cm^{-1}, logε = 1.2–1.5).Manifesting as a shoulder, it overlaps with the band of the calix[4]arene molecule at 276–283 nm (36230–35340 cm^{-1}), and the bands at 284–291 nm (35210–34360 cm^{-1}), which correspond to $\pi\rightarrow\pi^*$ transitions in the aromatic fragments of calix[4]arenes. The absorption spectra of the complexes in acetonitrile are also characterized by three bands in the range of 281–286 nm (35590–34970 cm^{-1}, logε = 3.78–3.86), 290–294 nm (34480–34000 cm^{-1}, logε = 3.74–4.17) and 304–310 nm (32890–32260 cm^{-1}, logε = 3.57–3.73). The bathochromic shift of the first two bands is 240–380 cm^{-1} compared to ligands, except for the complex with benzo-crown-derivative $[LuL^3Cl(CH_3CN]$ - $\Delta\lambda$ = =1260 cm^{-1} and 1210 cm^{-1}, for the first and second bands, respectively. The appearance of a band with a maximum in the region of 304–310 nm is characteristic of complexes of phenolic calix[4] arenes, when the metal ion replaces protons of OH groups. An increase in the number of glycol fragments in the azacrown ether substituent, as well as the presence of a carbonyl group in the link, practically does not affect the characteristics of the absorption bands of ligands and complexes (Table 2).

One of the conditions for effective *4f*-luminescence in the coordination compounds of lanthanides is the presence of excited singlet (S_1) and triplet (T_1) levels of ligands higher than the resonance levels of metals. The energy of excited levels was determined by studying the molecular fluorescence and phosphorescence spectra of solutions of the corresponding lutetium complexes (Table 2). The fluorescence spectra of Lu(III) complexes are similar and consist

of a wide band in the range of 390-450 nm with nanosecond range decay time. In comparison with the spectra of free ligands, they are characterized mainly by a bathochromic shift of the fluorescence bands (940–2880 cm^{-1}) and an almost 2.5–3 fold decrease in lif time. The difference is the complexes with 12-azacrown-4-derivatives L^1H_2 and L^5H_2, where a hypsochromic shift was recorded: 970 cm^{-1} and 1500 cm^{-1}, respectively, which is probably associated with a deviation of the coplanarity of the complex. Phosphorescence spectra recorded at 77K with a 50 ms time delay are presented as a wide band in the range of 430–470 nm. The energies of triplet states in lutetium complexes (E_T) were found to be in the range of 21650–22570 cm^{-1}. It should be noted that the energy difference between the S_1- and T_1-levels is small: 570–1300 cm^{-1}, which makes possible energy transfer from the S_1-level of the ligand to the radiative levels of lanthanide ions. The possibility of energy transfer from the S_1-levels to Ln(III) ions does not exclude the participation of T_1-levels in the sensitization of the lanthanide-centered luminescence, as well as energy back transfer from the radiative level of, for example, europium ions ($E(^5D_2)$ = 21500 cm^{-1}), which is energetically possible [15].

Table 2

Characteristics of absorption, fluorescence and phosphorescence spectra of lutetium complexes with azacrown ether-functionalized calix[4]arenes (C=1×10^{-3} M, CH_3CN).

Complex	λ_I, λ_{II}, λ_{III}, nm (log ε)			λ_{fl}, nm	τ, ns	E_S, cm^{-1}	λ_{phos}, nm	E_T, cm^{-1}	Δ_{E-T}, cm^{-1}
[LuL^{1}Cl-(CH_3CN)]	282 (3.83)	291 (3.82)	305 (3.72)	442	13.4	22620	454	22030	590
[LuL^{2}Cl-(CH_3CN)]	281 (3.84)	291 (3.81)	306 (3.70)	438	13.4	22830	452	22120	710
[LuL^{3}Cl-(CH_3CN)]	286 (4.28)	294 (4.17)	310 (3.69)	450	18.5	22220	462	21650	570
[LuL^{4}Cl-(CH_3CN)]	284 (3.78)	291 (3.73)	304 (3.57)	441	13.3	22680	457	21880	800
[LuL^{5}Cl-(CH_3CN)]	282 (3.79)	290 (3.74)	306 (3.68)	421	12.7	23750	443	22570	1180
[LuL^{6}Cl-(CH_3CN)]	282 (3.86)	292 (3.81)	307 (3.73)	427	12.1	23420	446	22420	1000
[LuL^{7}Cl-(CH_3CN)]	281 (3.82)	290 (3.77)	305 (3.62)	424	12.8	23590	449	22270	1320

The second, no less important condition for observing intense luminescence is the optimal energy gap between the triplet level of the ligand and the resonance level of the lanthanide ion. As already noted, for each element and each type of ligand, there is a certain optimal energy gap. Thus, for efficient energy transfer in europium complexes, the difference between the energy of the triplet level of the organic ligand and that of the resonant $^5D_0$ level of europium (III) ion should be between 2500–3500 cm^{-1} and for terbium (III) ion, 2500–4000 cm^{-1} [11, 15]. However, for example, for 3-methyl-1-phenyl-4-formyl-5-hydroxypyrazolates of Eu(III) and Tb(III) this regularity, so called «Latva's rule», is not observed, and an intense luminescence of terbium (III) ion is observed at an energy gap of only 200 cm^{-1}, and the europium complex does not exhibit luminescence at ΔE = 3450 cm-1. In this case, the luminescence intensity is relatively low due to the scattering of radiation energy at the high-lying sublevels of the ground state [16, 17].

It can be seen from the data obtained that excitation energy transfer from azacrown calix[4]arenes is possible to europium (III) ions ($^5D_0$ and $^5D_1$, E = 17250 cm^{-1} and 19000 cm^{-1}, respectively), terbium (III) (E($^5D_4$) = 20450 cm^{-1}), and to the low-lying excited levels of Ln(III) ions luminescent in the NIR region: neodymium (III) (E($^4F_{3/2}$) = 11500 cm^{-1}) and ytterbium (III) (E($^2F_{5/2}$) = 10300 cm^{-1}).

Nevertheless, in Nd(III) complexes the emission signal is very low, which is probably caused by the quenching effect of C-H- (2950 cm^{-1}) and C-N- (2250 cm^{-1}) vibrations in both the ligand and solvent molecules. In Eu(III), Tb(III), and Yb(III) complexes characteristic 4f-luminescence bands are observed.

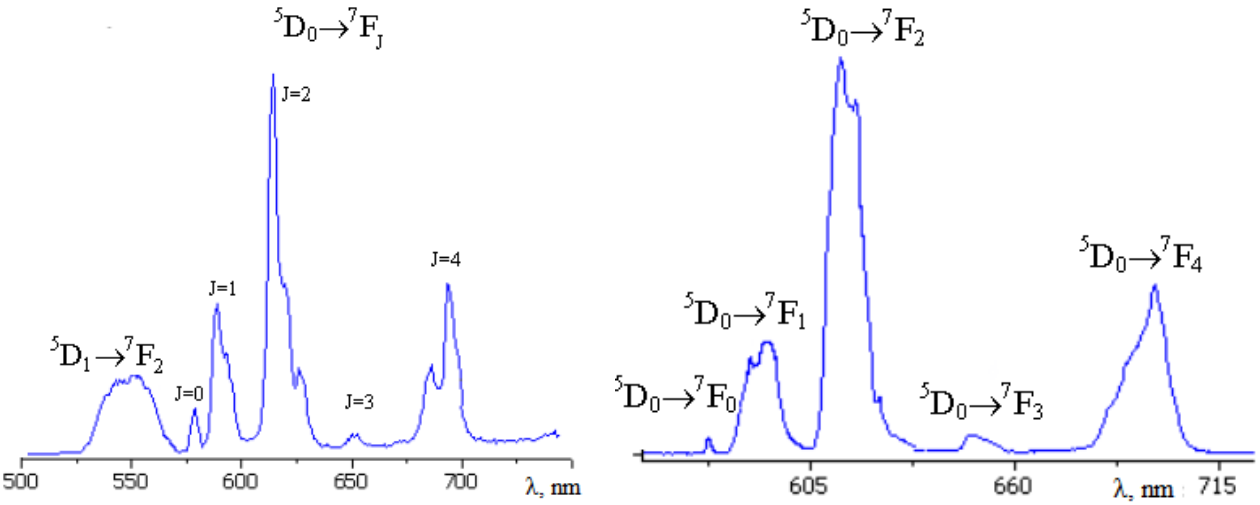

Fig. 4. *4f*-Luminescence spectra of complexes [EuL^{2}Cl(CH_3CN)] (left) and [EuL^{6}Cl(CH_3CN)] (right).

The coordination environment of the lanthanide ion was analyzed using emission spectra of Eu(III) compounds at 77K [14], whose luminescence occurred from the $^5D_0$ and $^5D_1$ levels. In the spectrum of [EuL^{2}Cl(CH_3CN)], there is a splitting into three components of

the bands corresponding to the transitions $^5D_0 \rightarrow ^7F_1$ and $^5D_0 \rightarrow ^7F_2$, which is characteristic of eight-coordinated europium ion (Fig. 4). This indicates that the type of the point symmetry group of the polyhedron of the Eu(III) ion is close to C_{2v} and the geometric structure of square antiprism, in accordance with the proposed structural formula. In the spectrum of the [EuL^{6}Cl(CH_3CN)] complex two intense bands corresponding to the transition from the $^5D_0$ level to the $^7F_2$ and $^7F_1$ levels undergo splitting into two components, which is a consequence of the distortion of the octahedral configuration of europium to C_{4v} type.

The excitation spectra of Tb(III) complexes (Fig. 5) are similar and consist of a wide band with maxima at 363–367 nm. Upon excitation at the maximum of this band, emission spectra are represented as a set of bands of low intensity ligand-centered emission in the 380–420 nm region as well as intense narrow bands of Tb-centered luminescence in the visible region. These peaks correspond to energy transitions: $^5D_4 \rightarrow ^7F_6$ (487 nm), $^5D_4 \rightarrow ^7F_5$ (542 nm), $^5D_4 \rightarrow ^7F_4$ (580 nm and 587 nm), $^5D_4 \rightarrow ^7F_3$ (620 nm), and $^5D_4 \rightarrow ^7F_2$ (643 nm and 650 nm). The quantum yield of terbium complexes is higher than that of the corresponding europium complexes (Table 3).

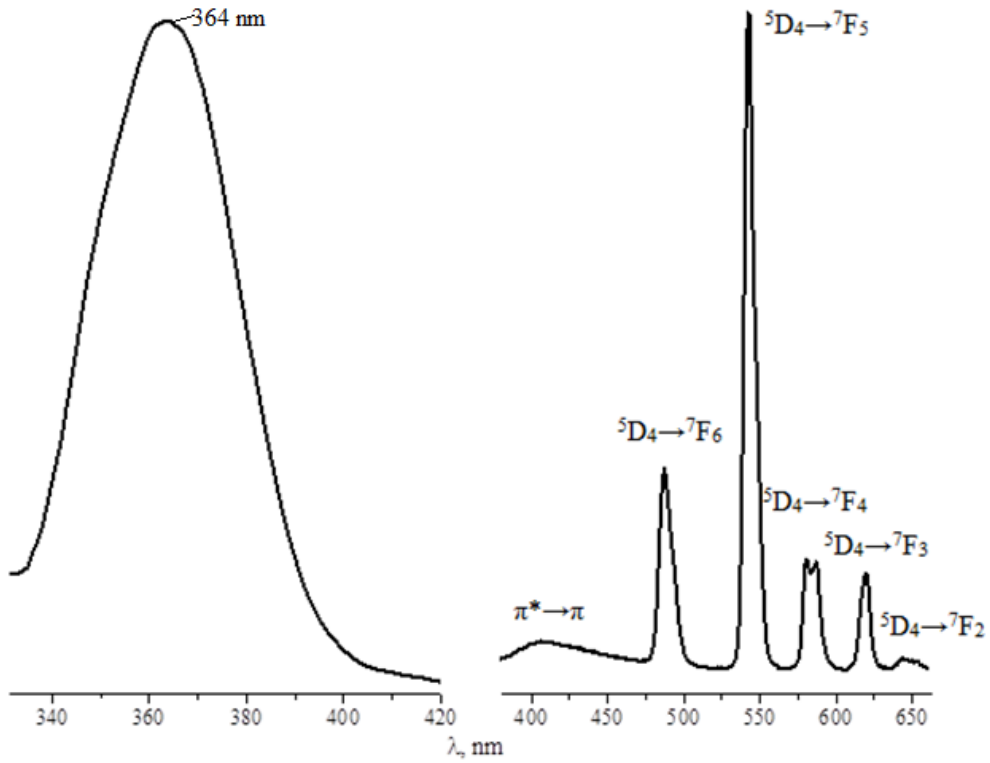

Fig. 5. Photoluminescence excitation (left) and emission (right) spectra of [TbL^{1}Cl(CH_3CN)].

The highest values of the quantum yields of *4f*-luminescence are observed for the complexes with the benzo-crown ether derivative L^3H_2, as compared to the corresponding complexes $[LnL^2Cl(CH_3CN)]$ and $[LnL^6Cl(CH_3CN)]$ (Table 3). It can be assumed that the presence of a benzene ring in the 15-azacrown-5 heterocycle leads to a redistribution of the electron density not only in the fragments of the substituent, but also in the molecule of this compound as a whole. This can be caused by an increase in the rigidity of the entire azacrown ether unit and a violation of the symmetry of the arrangement of oxygen atoms in the cycle. The number of coordinated solvent molecules in complexes was estimated and it was found that one solvent molecule is coordinated in all of the complexes.

Table 3

Characteristics of the *4f*-luminescence of Ln(III) complexes with azacrown ether-calix[4] arenes (C=1×10^{-4} M, methanol).

Complex	φ	τ(MeOH), mcs	τ(MeOD), mcs	q(MeOH)
$[EuL^1Cl(CH_3CN)]$	0.024	425	507	0.8
$[EuL^2Cl(CH_3CN)]$	0.023	398	469	0.8
$[EuL^3Cl(CH_3CN)]$	0.032	551	774	1.1
$[EuL^4Cl(CH_3CN)]$	0.019	428	552	1.1
$[EuL^5Cl(CH_3CN)]$	0.024	482	607	0.9
$[EuL^6Cl(CH_3CN)]$	0.017	419	551	1.2
$[EuL^7Cl(CH_3CN)]$	0.020	455	550	0.8
$[TbL^1Cl(CH_3CN)]$	0.432	858	2594	0.9
$[TbL^2Cl(CH_3CN)]$	0.448	853	3009	1.2
$[TbL^3Cl(CH_3CN)]$	0.452	915	3954	1.2
$[TbL^4Cl(CH_3CN)]$	0.421	795	2284	1.1
$[TbL^5Cl(CH_3CN)]$	0.290	871	2712	0.9
$[TbL^6Cl(CH_3CN)]$	0.293	823	2816	1.3
$[TbL^7Cl(CH_3CN)]$	0.386	805	2368	1.1

As can be seen, the optimal gap condition $\Delta E_{T1} \rightarrow 4f^*$ is not fulfilled for all Ln(III) ions. A particularly large difference between the energy of the triplet levels of the ligands and the energy of the resonant $^2F_{5/2}$ level, which reaches values greater than 10000 cm^{-1}, is observed in the case of ytterbium (III) complexes, which does not allow one to expect intense emission from the complexes. In the luminescence spectrum of the ytterbium complex, one band is observed due to the transition from the emitting level $^2F_{5/2}$ to the only ground level $^2F_{7/2}$; however, due to the distortion of the coordination polyhedron, the luminescence band splits with the appearance of three maxima at 982 nm, 1014 nm, and 1060 nm (Fig. 6). As in the case of Eu(III) and Tb(III) complexes, the highest quantum yield of Yb-centered luminescence was found in the complex with the benzo-crown ether derivative L^3H_2 (Table 4).

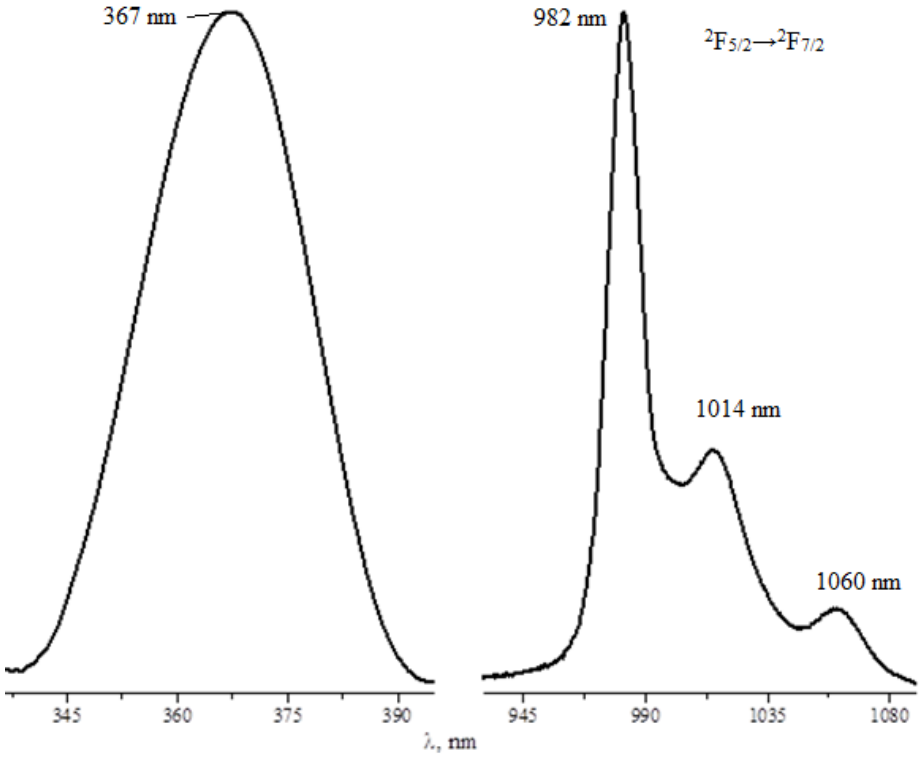

Fig. 6. Photoluminescence excitation (left) and emission (right) spectra of [YbL^{3}Cl(CH$_3$CN)].

Table 4

Values of the quantum yield of Yb(III) complexes with azacrown ether-calix[4]arenes.

Ligand	L^1H_2	L^2H_2	L^3H_2	L^4H_2	L^5H_2	L^6H_2	L^7H_2
φ	0.0042	0.0037	0.0054	0.0032	0.0037	0.0048	0.0041

CONCLUSIONS. Thus, methods of synthesis have been developed and the structure of coordination compounds of lanthanides with lower rim functionalized calix[4]arenes with azacrown ethers has been proposed. It was found that the values of the triplet levels of the ligands facilitate the transfer of excitation energy to the radiative levels of Ln(III) ions, which luminesce both in the visible and in the IR spectral regions. The most efficient *4f*-luminescence is observed for terbium-containing complexes with benzo-crown-derived ligands. It was found that the presence of macrocyclic substituents leads to a decrease in the energy of the singlet and triplet levels of calix[4]arenes.

ACKNOWLEDGEMENTS

The work was performed within the state budget theme «Prediction, molecular design and directed synthesis of new coordination compounds of metals of groups II and III of the Periodic Table with specified optical properties», state registration number: 0221U101322.

СТРУКТУРА ТА СПЕКТРАЛЬНО-ЛЮМІНЕСЦЕНТНІ ВЛАСТИВОСТІ ЛАНТАНІДВМІСНИХ КОМПЛЕКСІВ З АЗАКРАУН-КАЛІКСАРЕНАМИ

Смола С. С.[1], Русакова Н. В.[1], Алексеєва О. О.[1], Басок С. С.[1], Кіріченко Т. І.[1], Коровін О. Ю.[1], Малінка О. В.[2], Семенішин М. М.[1]

[1]Фізико-хімічний інститут ім. О. В. Богатського НАН України, 86, Люстдорфська дорога, Одеса 65080, Україна
[2]Одеська національна академія харчових технологій, 112, вул. Канатна, Одеса 65039, Україна
email: sssmola@gmail.com

Отримано комплекси лантанідів із калікс[4]аренами, заміщеними по нижньому ободу двома азакраун-естерними фрагментами. Розмір порожнини замісника варіювався від 4 до 6 гетероатомів. Комплекси аналізували за допомогою ІЧ, ЯМР, ESI-мас-спектроскопії. Припущено, що координація іонів Ln(III) відбувається за допомогою донорних атомів нижнього ободу, протиіон і молекула розчинника також є координованими. У комплексах Eu(III), Tb(III) та Yb(III) спостерігали лантанід-центровану характерну люмінесценцію. Найбільш ефективна 4f-люмінесценція спостерігається для тербійвмісних комплексів із лігандами, що містять бензокраун-похідні ліганди. Обговорюються шляхи сенсибілізації 4f-люмінесценції.

Ключові слова: комплекси лантанідів, калікс[4]арени, азакраунестери, люмінесценція.

REFERENCES

1. Othman A.B., Mellah B., Abidi R., Kim J.S., Kim Y., Vicens J. Complexing properties of pyrenyl-appended calix[4]arenes towards lanthanides and transition metal cations. *J. Incl. Phenom. Macrocycl. Chem.* 2020. **97**: 187–194. doi: 10.1007/s10847-020-00993-0.
2. Mokhtari B., Pourabdollah K. Application of Nano-Baskets for Extraction of Lanthanides. *J. Chem. Res.* 2012. **36**(12): 740–743. doi:10.3184/174751912X13527973569178.
3. Chinta J.P., Ramanujam B., Rao C.P. Structural aspects of the metal ion complexes of the conjugates of calix[4]arene: Crystal structures and computational models. *Coord. Chem. Rev.* 2012. **256**: 2762–2794. doi: 10.1016/j.ccr.2012.09.001.
4. Furphy B.M., Harrowfield J.M., Kepert D.L., Skelton B.W., White A.H., Wilner F.R.. Bimetallic lanthanide complexes of the calixarenes: europium(III) and tert-butylcalix[8]arene. *Inorg. Chem.* 1987. **26** (25): 4231–4236. doi: 10.1021/ic00272a018.
5. Delaigue X., Harrowfield J., Hosseini M., De Cian A., Fischer J., Kyritsakas N. Exoditopic receptors I: synthesis and structural studies on p-tert-butyltetramercaptocalix[4]arene and its mercury complexes. *J. Chem. Soc., Chem. Commun.* 1994. 1579–1580. doi: 10.1039/C39940001579.
6. Harrowfield J., Ogden M., Richmond W., White A. Lanthanide ions as calcium substitutes: a structural comparison of europium and calcium complexes of a ditopic calixarene. *J. Chem. Soc., Dalton Trans.* 1991. 2153–2160. doi: 10.1039/DT9910002153.
7. Alekseeva E.A., Basok S.S., Mazepa A.V., Luk'yanenko A.P. , Snurnikova O.V., Gren' A.I. *p-tert*-Butylcalix[4]arenes containing azacrown ether substituents at the lower rim as potential polytopic receptors. *Russ. J. Gen. Chem.*. 2013. **83**: 1738–1743. doi: 10.1134/S1070363213090181.
8. Alekseeva E.A., Basok S.S., Rakipov I.M., Ma-

zepa A.V., Gren' A.I. Specific features of the reduction of disubstituted amide derivatives of *p-tert*-butylcalix[4]arene. *Russ. J. Org. Chem.* 2013. 49: 1035–1041. doi: 10.1134/S1070428013070130.
9. Rudkevich D., Verboom W., Tol E. Calix[4] arene-triacids as receptors for lanthanides; synthesis and luminescence of neutral Eu^{3+} and Tb^{3+} complexes. *J. Chem. Soc. Perkin Trans.* 1995. 2: 131–134. doi: 10.1039/P29950000131.
10. Sabbatini N., Guardigli M., Mecati A., Balzani V., Ungaro R., Ghidini E., Casnati A., Pochini A. Encapsulation of lanthanide ions in calixarene receptors. A strongly luminescent terbium (3+) complex. *J. Chem. Soc., Chem. Commun.* 1990. 878–879. doi: 10.1039/C39900000878.
11. Latva M., Takalo H., Mukkala V.-M., Matachescu C., Rodriguez-Ubis J.C., Kankare J. Correlation between the lowest triplet state energy level of the ligand and lanthanide(III) luminescence quantum yield. *J. Lumin.* 1997. **75**: 149–169. doi: 10.1016/S0022-2313(97)00113-0.
12. Williams A.T.R., Winfield S.A., Miller J.N. Relative fluorescence quantum yields using a computer controlled luminescence spectrometer. *Analyst*. 1983. **108**: 1067–1071. doi: 10.1039/AN9830801067.
13. Horrocks W. deW. Jr., Sudnick D. R. Lanthanide ion probes of structure in biology. Laser-induced luminescence decay constants provide a direct measure of the number of metal-coordinated water molecules. *J. Am. Chem. Soc.* 1979. **101**(2): 334–340. doi: 10.1021/ja00496a010.
14. Binnemans K. Interpretation of europium (III) spectra. *Coord. Chem. Rev.* 2015; 295: 1–45. doi: 10.1016/j.ccr.2015.02.015.
15. Bünzli J.C.G., Choppin G.R. Lanthanide probes in life, chemical and earth sciences: Theory and practice. Amsterdam, Oxford, New York: Elsevier. 1989. 432.
16. Aulsebrook M.L., Graham B., Grace M.R., Tuck K.L., Lanthanide complexes for luminescence-based sensing of low molecular weight analytes. *Coord. Chem. Rev.* 2018. **375**: 191–220. doi: 10.1016/j.ccr.2017.11.018.
17. Parker D., Fradgley J.D., Wong K.-L. The design of responsive luminescent lanthanide probes and sensors. *Chem. Soc. Rev.*. 2021. **50**: 8193–8213. doi: 10.1039/D1CS00310K.

Стаття надійшла 14.11.2021.